

**AWARD NUMBER: W81XWH-14-2-0192**

**TITLE: Rapid Isolation and Detection for RNA Biomarkers for TBI Diagnostics”**

**PRINCIPAL INVESTIGATOR: Dr. Michael J. Heller**

**CONTRACTING ORGANIZATION: University of California, San Diego  
La Jolla, CA 92093**

**REPORT DATE: October 2015**

**TYPE OF REPORT: Annual**

**PREPARED FOR: U.S. Army Medical Research and Materiel Command  
Fort Detrick, Maryland 21702-5012**

**DISTRIBUTION STATEMENT: Approved for Public Release;  
Distribution Unlimited**

The views, opinions and/or findings contained in this report are those of the author(s) and should not be construed as an official Department of the Army position, policy or decision unless so designated by other documentation.

# REPORT DOCUMENTATION PAGE

*Form Approved*  
*OMB No. 0704-0188*

Public reporting burden for this collection of information is estimated to average 1 hour per response, including the time for reviewing instructions, searching existing data sources, gathering and maintaining the data needed, and completing and reviewing this collection of information. Send comments regarding this burden estimate or any other aspect of this collection of information, including suggestions for reducing this burden to Department of Defense, Washington Headquarters Services, Directorate for Information Operations and Reports (0704-0188), 1215 Jefferson Davis Highway, Suite 1204, Arlington, VA 22202-4302. Respondents should be aware that notwithstanding any other provision of law, no person shall be subject to any penalty for failing to comply with a collection of information if it does not display a currently valid OMB control number. **PLEASE DO NOT RETURN YOUR FORM TO THE ABOVE ADDRESS.**

<b>1. REPORT DATE</b> October 2015			<b>2. REPORT TYPE</b> Annual Report			<b>3. DATES COVERED</b> 30 Sep 2014 - 29 Sep 2015			
<b>4. TITLE AND SUBTITLE</b> Rapid Isolation and Detection for RNA Biomarkers for TBI Diagnostics”						<b>5a. CONTRACT NUMBER</b>			
						<b>5b. GRANT NUMBER</b> W81XWH-14-2-0192			
						<b>5c. PROGRAM ELEMENT NUMBER</b>			
<b>6. AUTHOR(S)</b>  Michael Heller  E-Mail: mheller@ucsd.edu						<b>5d. PROJECT NUMBER</b>			
						<b>5e. TASK NUMBER</b>			
						<b>5f. WORK UNIT NUMBER</b>			
<b>7. PERFORMING ORGANIZATION NAME(S) AND ADDRESS(ES)</b> University of California, San Diego 9500 Gilman Drive La Jolla, CA 92093-0621						<b>8. PERFORMING ORGANIZATION REPORT NUMBER</b>			
<b>9. SPONSORING / MONITORING AGENCY NAME(S) AND ADDRESS(ES)</b>  U.S. Army Medical Research and Materiel Command Fort Detrick, Maryland 21702-5012						<b>10. SPONSOR/MONITOR'S ACRONYM(S)</b>			
						<b>11. SPONSOR/MONITOR'S REPORT NUMBER(S)</b>			
<b>12. DISTRIBUTION / AVAILABILITY STATEMENT</b> Approved for Public Release; Distribution Unlimited									
<b>13. SUPPLEMENTARY NOTES</b>									
<b>14. ABSTRACT</b> Our project work is focused on using a new dielectrophoresis (DEP) microarray technology for rapid isolation and detection of brain-specific RNA and other biomarkers for TBI diagnostics and patient monitoring. Initial year one project goals include developing DEP techniques for isolation of circulating cell-free (ccf) RNA from glioblastoma exosomes and TBI samples ( <i>IRB dependent</i> ); methods for on-chip fluorescence detection of exosomes, RNA, and other biomarkers; methods for isolation of mRNA and miRNA from exosomes; and development of RT-PCR techniques and specific primers for identifying brain-specific mRNAs, miRNAs and other biomarkers. We have been successful in demonstrating DEP isolation of glioblastoma exosomes from 50 $\mu$ L of un-diluted plasma in fifteen to twenty minutes. We also showed tri-color fluorescent detection of the isolated exosomes (red fluorescence), ccf-RNA (green fluorescence) and ccf-DNA (blue fluorescence). Finally, glioblastoma-specific mRNAs for EGFRvIII as well as more universal beta-actin biomarkers were identified by RT-PCR carried out on ccf-RNA extracted from the exosomes.									
<b>15. SUBJECT TERMS</b> Nothing Listed									
<b>16. SECURITY CLASSIFICATION OF:</b>						<b>17. LIMITATION OF ABSTRACT</b>	<b>18. NUMBER OF PAGES</b>	<b>19a. NAME OF RESPONSIBLE PERSON</b>	
<b>a. REPORT</b>	<b>b. ABSTRACT</b>	<b>c. THIS PAGE</b>			USAMRMC				
Unclassified	Unclassified	Unclassified	Unclassified		57	<b>19b. TELEPHONE NUMBER</b> (include area code)			

# Table of Contents

	<u>Page</u>
<b>1. Introduction .....</b>	<b>4</b>
<b>2. Keywords .....</b>	<b>4</b>
<b>3. Accomplishments .....</b>	<b>4</b>
<b>4. Impact .....</b>	<b>37</b>
<b>5. Changes/Problems. ....</b>	<b>38</b>
<b>6. Products .....</b>	<b>39</b>
<b>7. Participants &amp; Other Collaborating Organizations .....</b>	<b>40</b>
<b>8. Special Reporting Requirements .....</b>	<b>42</b>
<b>9. Quad Chart .....</b>	<b>43</b>
<b>10. Appendices .....</b>	<b>44</b>

**ANNUAL - YEAR ONE REPORT – Sept. 30, 2015**  
**W81XWH-14-2-0192 - Log #13212004**  
**“Rapid Isolation and Detection of RNA Biomarkers for TBI Diagnostics”**

## **1. INTRODUCTION**

Current limitations for detection and accurate diagnosis of Traumatic Brain Injury (TBI) in point-of-care (POC) settings pose an ongoing capability gap. For soldiers in training and combat, rapid diagnosis and monitoring of mild, moderate or repeated TBI is of absolute importance. Any brain trauma in the field may not only have serious short-term implications, but also may progress to chronic and debilitating long-term physiological and psychological problems for soldiers and veterans. Our project work is focused on using a new dielectrophoresis (DEP) microarray technology for rapid isolation and detection of brain-specific RNA and other biomarkers for TBI diagnostics and patient monitoring. Initial year one project goals include developing DEP techniques for isolation of circulating cell-free (ccf) RNA containing exosomes (glioblastoma cell model) from blood, plasma, serum or CSF; methods for on-chip fluorescent detection of exosomes, RNA and other biomarkers; methods for isolation of mRNA and miRNA from the isolated exosomes; and the development of RT-PCR techniques and specific primers and probes for identifying brain-specific mRNAs, miRNAs and other biomarkers. Next phase (Year One – Year Two) goals include: on-chip fluorescent detection of RNA (exosomes) from moderate to severe TBI blood samples; and development of an algorithmic approach for correlating RNA detections with TBI severity. Final project (Year Two) goals include demonstrating rapid DEP isolation and RT-PCR detection of specific RNA (mRNA & miRNA) biomarkers for severe, moderate and mild TBI; determining which RNAs or other biomarkers can be used for differentiating types of brain damage; and demonstrating on-chip (DEP device) identification of RNA and other biomarkers. Completion of the project objectives will position the DEP technology for development of a fully integrated, robust, portable sample-to-answer POC system for TBI diagnostics and patient monitoring.

## **2. KEYWORDS**

Traumatic brain injury, brain-specific biomarkers, RNA, exosomes, extracellular vesicles, proteins, dielectrophoresis, molecular diagnostics, sample-to-answer, point-of-care,

## **3. ACCOMPLISHMENTS**

### **3.1 Major Project Goals and Objectives**

**First Specific Aim and Tasks (Year 1)** – Design, develop and test eight sets of Polymerase Chain Reaction (PCR) primers for brain specific and TBI related RNAs; four sets for brain-specific messenger RNA (mRNA) and four sets for confirmed small non-coding RNA including micro RNAs (mi-RNAs) and/or small nucleolar RNAs (sno-RNAs). Initial brain-specific mRNA targets may include, but are not limited to, neurofilament protein (NFp), glial fibrillary acidic

protein (GFAP), neuron-specific enolase (NSE), and brain IL-1b. The initial non-coding RNA targets may include, but are not limited to, sno-RNAs ACA48, HBII-239, U91 and miRNA Has-miR-671-5p. Positive controls will be normal blood or plasma or CSF samples (no injury or pathology), which have been spiked with generic RNA (not brain- or TBI-related), as well as blood or plasma or CSF samples which have been spiked with disrupted cells or brain related exosomes and/or extracted RNA from U87 Glioblastoma cell line cultures which overexpress a mutant variant of EGFR called EGFRvIII. High conductance DEP (HC-DEP) isolation and detection of RNAs will be carried out and compared to the conventional “gold standard” methods for RNA isolation. This will include using a commercially available Exiqon miRCURY RNA isolation kit, which isolates total RNA, including mRNA as well as smaller miRNA. Detection will include on-chip fluorescent imaging of RNA stained with an RNA specific dye, which is isolated on the HC-DEP microarray; as well as fluorescence analysis and quantification of RNA eluted from the HC-DEP microarray devices. RT-PCR and PCR amplification and analysis will be carried out on both the isolated RNA from the HC-DEP microarray devices and by the conventional gold standard methods. This initial work can be carried out using commercially available blood or plasma samples, while additions and/or changes related the TBI grant work are made and approved for Dr. Clark Chen’s present IRB at the UCSD Moores Cancer Center. Also, begin submission of a TBI project related IRB at NMCS. Months 1 to 6.

**Second Specific Aim and Tasks (Year 1)** - Using HC-DEP, isolate circulating cell-free (ccf) RNA from at least 12 moderate/severe TBI blood and/or plasma and/or CSF samples (annotated and/or fresh samples obtained from Dr. Clark Chen, at the UCSD Moores Cancer Center); and carry out on-chip fluorescent detection of the ccf-RNA using RNA-specific dyes. Normal blood/plasma/CSF samples will be used as negative controls, and samples spiked with RNA as positive controls. Months 6 to 9

**Third Specific Aim and Tasks (Year 1)** – Using HC-DEP, carry out the isolation of ccf-RNA from at least 15-20 moderate/severe TBI blood, plasma or CSF samples. Use the reverse transcriptase (RT) reaction and PCR procedures to determine the presence of brain-specific RNA (mRNA, miRNA, etc.) in the TBI samples. Normal blood samples will be used as negative controls, and samples spiked with known RNA sequences will be used as positive controls. Quantitative fluorescence analysis will be carried out on eluted ccf-RNA isolated from TBI samples and normal samples by HC-DEP, and compared to ccf-RNA isolated from TBI and normal samples isolated by the conventional gold standard method. Carry out PCR analysis on eluted ccf-RNA isolated from TBI samples and normal samples by HC-DEP, and compare to results for ccf-RNA isolated from TBI and normal samples isolated by the conventional gold standard method. Months 9 to 12

**Fourth Specific Aim and Tasks (Year 1)** - Based on RNA detection results received from UCSD’s high conductance dielectrophoresis (HC DEP), and based on associated patient/victim assessments from the UCSD Medical Center and the Naval Medical Center San Diego, Raytheon shall perform correlation of RNA detections with TBI severity to support proof-of-principle. Raytheon shall develop a top level algorithmic approach for translating diagnostic results into predictions of outcome for the patient/victim. The approach will focus on the RNA detections from this program. However, the approach shall be structured to incorporate additional diagnostic inputs as they become available in the future. (Note that this task is to develop an approach only. Actual algorithm design and coding will be reserved for follow-on programs.) Month 6 to 12

**First Milestone (Year 1)** – Complete the design and testing of PCR primers for four brain-specific and/or TBI-specific messenger RNAs (mRNAs), and for four brain- and/or TBI-specific small noncoding RNAs (miRNAs, snoRNAs, etc.). (Months 0-6)

**Second Milestone (Year 1)** – Demonstrate fluorescent detection of ccf-RNA isolated from severe TBI blood samples by HC-DEP. (Months 0-6)

**Third Milestone (Year 1)** – IRB changes for UCSD approved (Month 6)

**Fourth Milestone (Year 1)** – Raytheon: Receiver Operating Characteristic (ROC) results on proof-of-principle data from HC DEP and neurotrauma specialists assessments. Documentation of approach in first annual report. (Month 12)

**Fifth Milestone (Year 1)** – Demonstrate two or more brain-related and/or TBI-related RNA biomarkers were present in the ccf-RNA isolated from severe TBI blood samples using HC-DEP. This represents a key first-year milestone demonstrating a basic proof of principle. (Month 12)

### 3.2 Accomplished Goals

The following describes the accomplishments during the first year's work including highlights from 1<sup>st</sup>-3<sup>rd</sup> quarters, and a detailed description of the 4<sup>th</sup> quarter's new work. Most of the year one goals (specific aims and tasks) not related to final IRB approval and the use of TBI samples have been accomplished. While our milestone for obtaining the UCSD IRB was achieved (May 2015), the IRB has not yet been approved by HRPO (ORP/USAMRMC); therefore, we could not complete the project goals requiring human TBI samples. Nevertheless, upon IRB final approval, we are in position to immediately proceed and complete 1<sup>st</sup> year goals using TBI samples. Because of our success on the other important project goals, we should be able to complete this work on initial TBI samples within 3-4 weeks of IRB final approval.

By way of definitions for this report the term circulating cell-free (ccf) RNA is used to describe any RNA found outside of the cell and circulating in the blood (plasma, serum), lymph fluid or CSF. Ccf-RNA can include message (m) RNA, micro (mi) RNA, ribosomal (r) RNA or any other type of RNA biomarkers. It is now generally accepted by biomedical researchers in this area that ccf-RNA (mRNA, miRNA, rRNA) is most often found encapsulated within exosomes or other extracellular vesicles (ECV), and/or associated with proteins, as is the case for some miRNAs. Present techniques that are available for the isolation of exosomes/ccf-RNA from blood and other clinical samples still remain extremely long and laborious processes. One of the key technical goals for our TBI project work was to show that the DEP based technology being developed is effective for rapid isolation of exosomes and associated ccf-RNA. To this end, we have been successful in demonstrating the DEP isolation of glioblastoma exosomes from 50  $\mu$ L of plasma in about fifteen twenty minutes. We also showed tri-color fluorescent detection of the isolated exosomes (red fluorescence), ccf-RNA (green fluorescence) and ccf-DNA (blue fluorescence). Finally, glioblastoma-specific mRNAs for EGFRvIII and  $\beta$ -actin biomarkers were identified by RT-PCR carried out on ccf-RNA extracted from the exosomes. These results represent some of the key highlights for the first year project work.

## **IRB Protocol Activity and Status**

Our IRB #150010 for obtaining TBI samples (blood, plasma, serum, CSF) from human subjects was approved by the University of California San Diego Human Research Protections Program Committee on May 21, 2015. All documents were then sent to Brian Garland (CTR USARMY MEDCOM) (June 23 & July 6, 2015). Dr. Garland then forwarded the documents to Ms. Rochelle N. Day, B.A., CIP Human Subjects Protection Scientist (General Dynamics Information Technology) Human Research Protection Office (HRPO) Office of Research Protections (ORP) United States Army Medical Research and Materiel Command (USAMRMC) Fort Detrick, Maryland. On August 28, 2015 further requirements and questions regarding the IRB (HRPO Log Number A-18340 ) were received from Ms. Rochelle N. Day, B.A., Human Research Protection Office (HRPO). On September 18, 2015 we (Dr. MJ Heller, PI and Dr. Clark Chen, CoPI) sent the requested information back to Ms. Rochelle N. Day, B.A at the Human Research Protection Office (HRPO). Presently, we are waiting for final approval of our IRB by HRPO.

## **First Quarter Highlights (Oct-Dec 2014)**

Demonstration of DNA and RNA isolation, collection and fluorescent detection using DEP microarray devices:

- We showed that free RNA and DNA from cell lysates in PBS buffer can be isolated by DEP and detected by fluorescence in the high-field region around the DEP microelectrodes.
- We showed that the free DNA from the cell lysates can be isolated by DEP when spiked into undiluted human plasma. However, the free RNA is rapidly destroyed by endogenous RNase activity within minutes of being spiked into the human plasma. This means that most ccf-RNA in circulation (blood) must be in some protected form, such as inside *exosomes or other extracellular vesicles (ECV)*. Again, this is now generally accepted by most researchers working in the ccf-RNA area, and emphasizes the importance of exosome and ECV isolation as the first step in obtaining ccf-RNA.

Cell lines for exosomes/ccf-RNA (mRNA and miRNA) and RT-PCR Primers

- U-87 MG (glioblastoma), U87-EGFRvIII (glioblastoma cell line expressing EGFRvIII mutation), U118 (glioblastoma), U2OS (bone osteosarcoma), A549 (lung carcinoma), HeLa (cervical adenocarcinoma) were obtained.
- Primers were designed and tested for brain-specific mRNA targets: FABP, GFAP, NSE, MBP, S100B.

## **Second Quarter Highlights (Jan-Mar 2015)**

Demonstration of DEP isolation and collection of exosomes containing ccf-RNA from plasma:

- We demonstrated that exosomes collected from the glioblastoma cell line (U87-EGFRvIII) can be spiked into undiluted human plasma, and then recovered using our DEP microarray device and techniques. The exosomes were pulled down to the DEP microelectrode edges, washed, and recovered (Figure 1). The exosomes and ccf-RNA were stained with fluorescent dyes for detection and content. We found that only some exosomes appear to contain RNA.

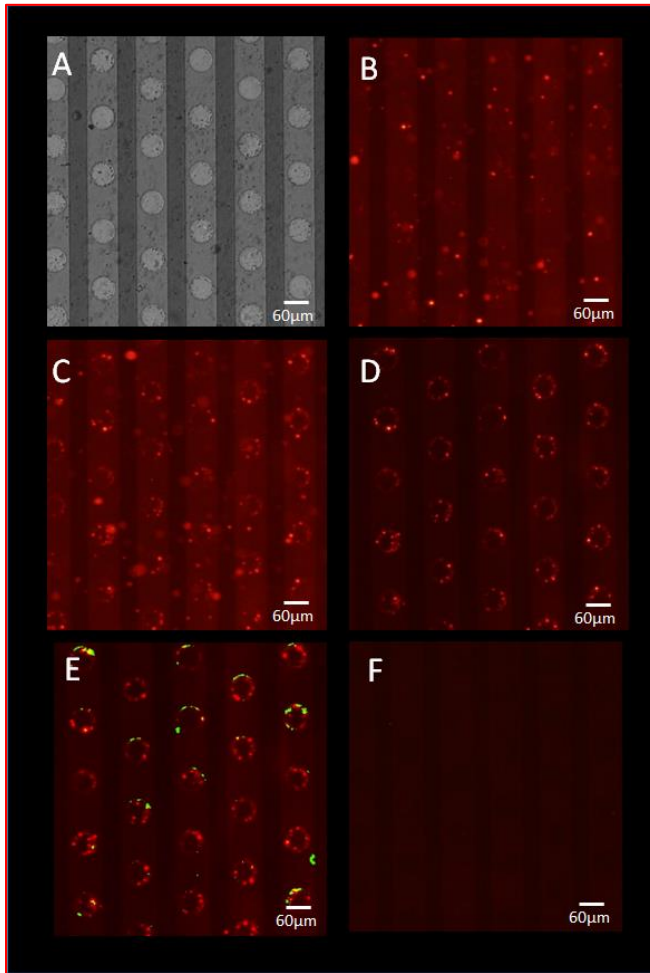


**Figure 1** – Images at different stages of DEP purification and recovery of spiked glioblastoma exosomes from undiluted human plasma. **A** - Bright-field image of the DEP microarray (chip) surface. Each of the circles is an individual microelectrode. The electric field is strongest at the edges of the microelectrodes and this is also where the DEP strength is the highest. **B** - A fluorescence view of the surface of the DEP chip. The exosomes have been labeled with the red PKH26 dye. Larger aggregates of the exosomes are visible as red dots. **C** - After 10 min. of DEP field application, the exosomes are collected around the edge of the electrodes, forming a fluorescent ring. **D** - The bulk plasma and uncollected exosomes are removed with a 10 min. wash with 1X TE buffer leaving the captured exosomes in the DEP high field regions in place. **E** - The captured exosomes were stained with RNA Select fluorescent dye that is specific for RNA and is membrane permeable. The RNA Select is shown in green in this composite image. Only

about 20%-30% of the exosomes actually stained for RNA content. **F** - The isolated exosomes were pushed off the surface of the chip by reversing the DEP force and were recovered for further analysis.

### Third Quarter Highlights (Apr-Jun 2015)

Characterization of the ccf-RNA extracted from exosomes collected by DEP:

- Sufficient ccf-RNA containing exosomes were recovered by DEP to allow for the ccf-RNA content to be analyzed using RT-PCR showing that the cell-specific EGFRvIII mRNA biomarker characteristic of the U87-EGFRvIII cell line was present (Figure 2), as well as mRNA for the general housekeeping gene for  $\beta$ -actin (Figure 3).



- We also demonstrated that the exosomes can be opened (lysed) releasing ccf-RNA for analysis by using heat and Tween surfactant, which will streamline the overall analysis process by avoiding the use of time-consuming kits to lyse the exosomes (Figure 4).

**Figure 2** – Gel analysis of RT-PCR followed by endpoint PCR performed on the DEP recovered exosomes using primers specific for the mRNA EGFRvIII mutation expressed by the U87-EGFRvIII cell line. The negative control and the plasma from a normal healthy donor that did not have exosomes spiked into it did not show any RNA coding for the EGRFvIII mutation. The DEP method recovered sufficient amounts of exosomes and ccf-RNA content to show that mRNA-specific biomarkers for the cell line of interest can be detected.

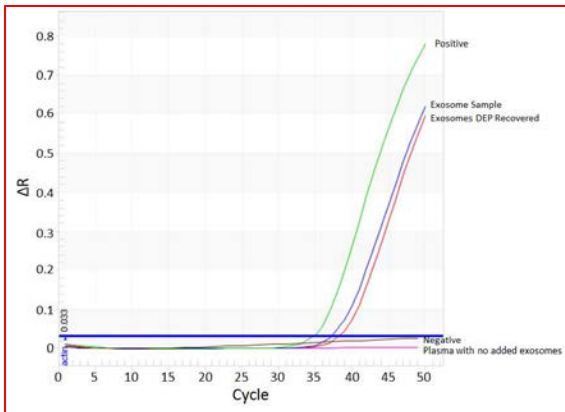


**Figure 3** – RT-PCR followed by qPCR analysis using RNA primers for  $\beta$ -actin from exosomes recovered using DEP. The exosome sample before spiking into the plasma came up showing that  $\beta$ -actin mRNA was present in the exosome sample. Two replicate samples of exosomes recovered from undiluted plasma using the DEP technique show the presence of mRNA coding for  $\beta$ -actin. Negative control plasma (no exosomes) did not show presence of  $\beta$ -actin mRNA.

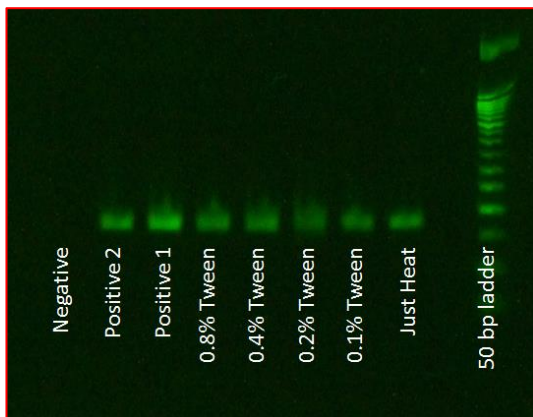


**Figure 4** - Gel analysis of RT-PCR followed by endpoint PCR performed on the exosomes using primers specific for the EGFRvIII mRNA biomarker expressed by the U87-EGFRvIII cell line. These exosomes were not lysed by use of kit, but rather, the RNA was released by heating the exosomes and using Tween20 surfactant in increasing concentrations to disrupt the exosome membrane. These techniques were successful for releasing the EGFRvIII coding mRNA for analysis.

## Fourth Quarter New Results (July-Sept 2015)

Detection and characterization of the exosome/ccf-RNA/ccf-DNA material collected by DEP

- We now have demonstrated three-color fluorescent detection, where ccf-DNA (blue) and exosomes (red) containing ccf-RNA (green) were simultaneously isolated into the DEP high-field regions of the microelectrodes (Figure 5).
- We have also further characterized the exosomes produced by the glioblastoma cell line (U87-EGFRvIII) using standard transmission electron microscopy (TEM) techniques (Figure 6). These exosomes were previously stained with red fluorescent lipid membrane dye for visualization (Figure 1 and 5).
- Additionally, we have characterized the region of collection around the DEP microelectrode edge using scanning electron microscopy (SEM) as shown in Figure 7. This shows the nature of the surface of collected material which is loosely aggregated and very porous. It also defines the effective DEP high-field region where the important biomarker materials (exosomes, ECVs, ccf-RNA, ccf-DNA and protein aggregates) are collected.
- This and our earlier work on DEP isolation of glioblastoma exosomes and associated ccf-RNA from plasma are being incorporated into a manuscript for the ACS Nano Journal. We believe that this represents very fundamental work that not only applies to our TBI project proposal goals, but will also be extremely valuable to the biomedical research community involved in cancer and other disease-related exosome and ccf-RNA work.

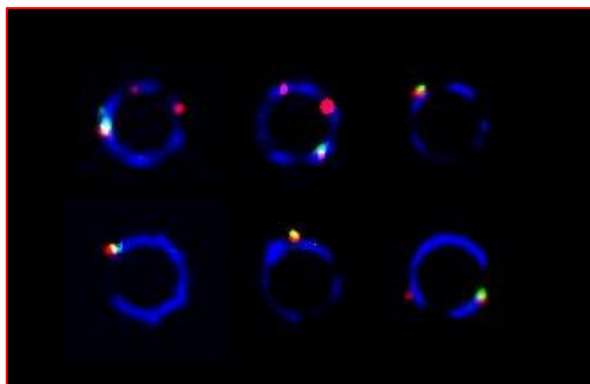


**Figure 5** – Multi-color fluorescence analysis of exosomes, ccf-RNA and high molecular weight DNA spiked into the plasma samples. Six representative microelectrodes are shown where blue shows the DNA stained with DAPI, red shows the exosomes, and green shows where RNA Select stained RNA present in the exosomes. As in Figure 1, not all of the exosomes co-stained for ccf-RNA.

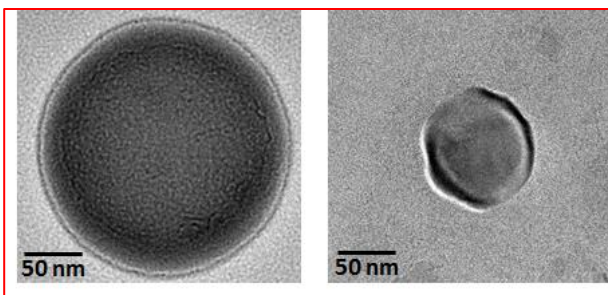


**Figure 6** – TEM images of glioblastoma exosomes recovered from cell culture media. The sizes ranged from 50 to 100 nm.

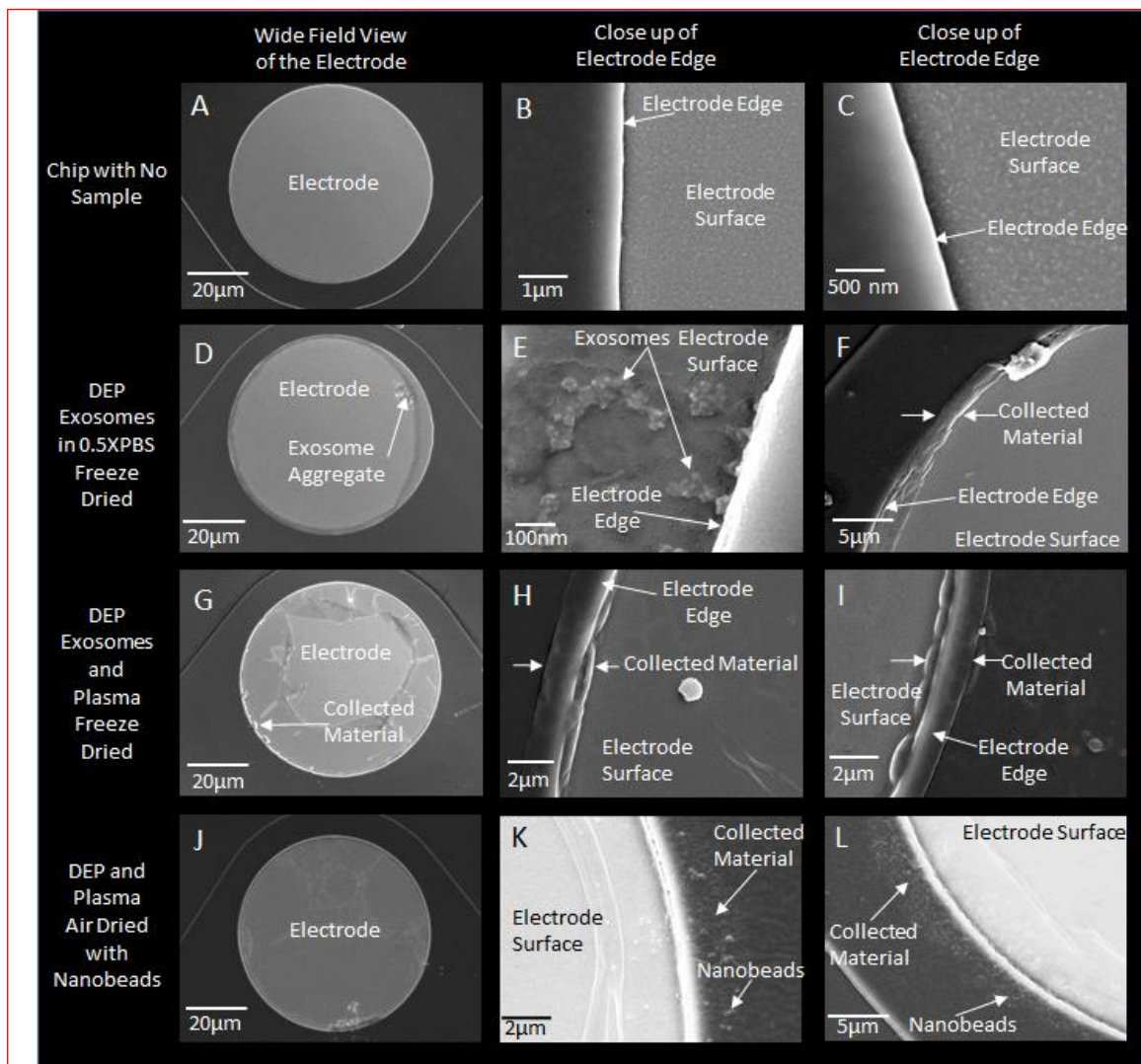


**Figure 7** – Scanning electron microscopy images of the DEP microelectrode array surface before and after DEP collection from human plasma and washing. **A** – A view of a microelectrode from a chip before it has been exposed to plasma. **B and C** - A magnified image of the edge between the microelectrode and the silica surface of the chip. **D** - A microelectrode after collection and washing of exosomes from 0.5X PBS (freeze drying preparation). Image shows hydrogel layer on the surface of the electrode has separated from the platinum electrode underneath creating a surface texture. **E** - Magnified view of the microelectrode edge showing the collection of nanoparticles from the exosome sample. **F** - Another image of collected material from the exosome sample. This material most likely includes proteins and lipids from the original cell culture media. **G** - Microelectrode after collection and washing of exosomes from a spiked undiluted human plasma sample. The hydrogel layer has been ruptured possibly from the freeze drying process. **H and I** - Magnified image of the microelectrode edge. Material from the plasma including DNA and the exosomes (Figure 5) are shown here collected together at the curved smooth surface of material indicated between the arrows. This material hides the exosomes within it. The freeze drying process has preserved the original shape of the collected material. **J**

- Surface of the electrode after collection of 110 diameter polystyrene nanobeads from undiluted human plasma prepared using an air drying process. **K and L** - A magnified image of the microelectrode edges. When allowed to air dry the collected material collapsed into a thin film showing the polystyrene nanobeads within it.

Design and testing of more mRNA biomarker primer sets:

- When we redesigned and optimized our primers and protocols for the EGFRvIII, we were able to detect lower amounts of mRNA transcripts.
- Because we are working with small sample volumes containing limited amounts of genetic material (mRNA), sensitive and specific primers (and probes) are very important for the project.

Preliminary work on releasing encapsulated genetic material (mRNA, miRNA) from exosomes without using Qiagen or Exiqon kits.

- When there are higher levels of mRNA, RT-PCR amplification works very well. However, for very low levels of mRNA, efficient protocols for releasing all the RNA materials from the samples are required for effective RT-PCR and qPCR analysis.

Preliminary work on microRNA: miR-16 and miR-765 biomarkers

- We were able to show detection of miR-16 from total RNA isolation from glioblastoma cell line (**Figure 8**)
- Taken from the grant proposal:

***Redell J.B., Moore A.N., Ward N.H. III, Hergenroeder G.W. and Dash P.K. Human traumatic brain injury alters plasma microRNA levels. J. Neurotrauma 2010, 27, 2147-2156. <http://online.liebertpub.com/doi/full/10.1089/neu.2010.1481>***

*The key findings from this study are: (1) the plasma level of miR-765 is significantly elevated, while miR-16 and miR-92a levels are significantly decreased, as determined by qRT-PCR analysis of plasma of patients with severe TBI compared to healthy volunteers; (2) altered miR-16, miR-92a, and miR-765 plasma levels were also observed when severe TBI patients were compared to orthopedic injury patients; (3) a biomarker signature, consisting of miR-16, miR-92a, and miR-765, had 100% sensitivity and specificity for discriminating severe TBI from healthy volunteer; (4) in contrast to that seen in severe TBI, the plasma levels of miR-16 and miR-92a were significantly elevated in mild TBI patients; and (5) the plasma levels of miR-16 and miR-92a can be used to discriminate mild TBI patients from healthy volunteer with a diagnostic accuracy of 0.81.*

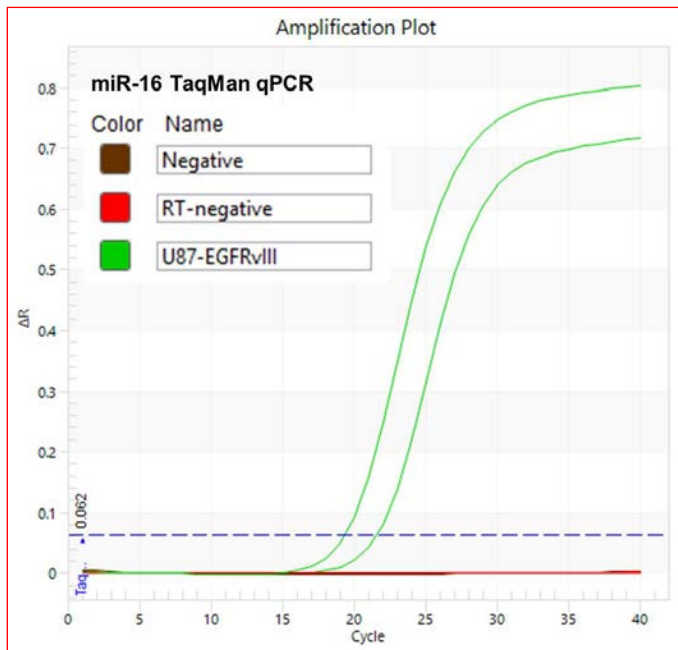


**Figure 8** - Preliminary work on microRNA showing detection of miR-16 from total ccf-RNA isolation from glioblastoma cell line.

## New DEP MicroArray (Chip) and System Protocols

We have developed a new protocol for running the DEP microarrays (chips) that is more time efficient, the procedure is described below:

### System Setup

1. Turn on the fluorescent light source
2. Turn on the computer
3. Turn on the syringe pump
4. Turn on the signal generator
  - a. You need to setup the signal generator to work with the amplifier using the following menu selections: Utility/Output setup/High Z/Done
5. Turn on the amplifier (make sure to turn the amplifier on before connecting the chip).
  - a. Make sure the amplifier is set to 1X, Low bandwidth, and AC+DC.
6. Take the plunger out of the wash buffer reservoir
7. If the hydraulic syringe system is older than 2 or 3 days then replace the syringes.
  - a. Remove the entire assembly from the microscope & syringe pump and place on bench.
  - b. Push on the 1 mL syringe to force the two syringes out of the 50 mL conical tube.
  - c. Loosen the screws on the Plexiglas connector to allow the two syringe plungers to be removed. You don't have to take the screws out all the way.
  - d. Throw the old syringes into the sharps container

- e. Make sure to move the plunger on each new syringe in and out a couple times to make sure the rubber is not sticking.
- f. Replace with new syringes and tighten the screws down until you feel some resistance, but not too much otherwise it will crack the plastic.
- g. Remember to transfer the extra cross piece for the old 5 mL syringe to the new one.
- h. Replace the connected syringes into the 50 mL conical tube using screw driver to make sure the cross piece on the 5 mL syringe goes into the slots in side of the tube and locks in place
- i. Pull the 1 mL syringe through the conical tube until its edges lock into the slots at the end of the conical tube. You want to make sure the two syringes are stable
- j. Replace the 5 mL syringe that will go into the syringe pump (free 5ml syringe)
- k. Fill the 5 mL syringe that goes into the syringe pump all the way with water.
- l. Force the water into the 5 mL syringe in the conical tube
- m. Hold the 5 mL syringe in the conical tube pointing up and pull all the air and water into the free 5 mL syringe.
- n. Empty the air out of the free 5 mL syringe
- o. Replace the system in the holder and the free 5 mL syringe into the syringe pump tightening the holder screw

### DEP Microarray (Chip) Setup

8. Select chip and record it in the log
9. Load chip into DEP system (shown in Figure 9) and screw down the lid with the nuts firmly to keep it in place

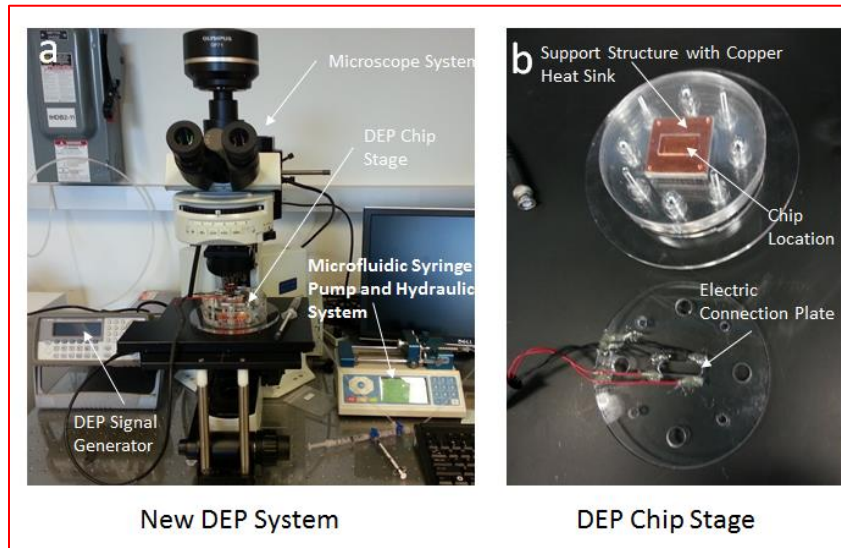


**Figure 9** – The DEP system setup has now been modified to be able to accommodate both 4 pin style DEP microarray (chips) and 6 pin DEP microarray (chips) that are manufactured by Biological Dynamics (San Diego, CA). This allows us the ability to use all the different DEP chip styles manufactured by the company for maximum versatility.

## Plasma Sample Preparation

10. Prepare the plasma sample. It should have a final total volume of at least 40  $\mu\text{L}$ 
  - a. Usually we prepare 50  $\mu\text{L}$  of plasma sample (49  $\mu\text{L}$  of plasma sample and 1  $\mu\text{L}$  of red fluospheres beads diluted 100X in 0.5X PBS)

## Loading Plasma Sample

11. Use the 1 mL pipette to put the plasma sample into the chip. It may take several times of injecting and removing the plasma sample to get it to completely fill the chip.
12. Insert a red blunt needle into a Tygon tube about 6 inches in length
13. Bring the chip/DEP setup and the tube from step 12 to the microscope. The wires from the DEP setup should face left towards the amplifier
14. Open the valve on the wash buffer reservoir to make sure that all the air bubbles are out of the tube. Let a couples of drops fall on the tissue paper.
15. Close the wash buffer reservoir value
16. Then with the sharp tweezers insert the wash buffer tube into the left input port of the chip.
17. Connect the red blunt needle to the syringe system.
18. The with the sharp tweezers insert the tube from step 17 into the right hand port on the chip
19. Place the DEP setup into the microscope stage.
20. Connect the DEP setup to the amplifier.

## Running the DEP

21. The settings on the signal generator should be 15 KHz, and start with 11.5 Vpp.
22. Start the signal generator by pressing the Output button so that it turns green.
  - a. You can increase the voltage setting as high as 15.5 Vpp as long as the chip does not start excessive bubbling. This can speed pretreatment of the chip.
23. The chip electrodes should start pre-treating within a few minutes
24. Let the chip collect for 10 min. Take various bright-field and fluorescent image pairs across the chip to get an idea of how the chip is collecting. Usually one bright-field and fluorescence-paired image for each section of the chip

## Washing the Chip

25. Open the valve on the wash buffer reservoir
26. After 10 min of DEP collection you can then begin the wash. On the syringe pump you will need to run at 100  $\mu\text{L}/\text{min}$  for a total of 1000  $\mu\text{L}$  (default settings) because of the hydraulic system reducing the speed by 5X. This will pull a total of 200  $\mu\text{L}$  of fluid running at 20  $\mu\text{L}/\text{min}$  through the chip.
  - a. Run the syringe pump until it has withdrawn about 150  $\mu\text{L}$  of fluid. If the wash has not started moving through the chip yet then you will need to release the built up vacuum in the syringe in the syringe pump by connecting it to the manual syringes.
  - b. Switch the hydraulic system over to manual mode to manually get the flow going through the chip. Pull back on the plunger just a little bit and hold it to see if flow starts. If not then pull back a little further.

- c. Once you get fluid moving you can then switch over to the syringe pump again.
- d. Start the syringe pump again and monitor for flow to occur within 1 min in the chip

### **Push Off/Sample Release**

27. After 1000  $\mu\text{L}$  has been moved by the syringe pump you can stop the pump
28. Pull out the two hoses from the chip using the tweezers
29. Turn off the Output of the signal generator so the green light turns off
30. Reset the signal generator to 5 Hz and 20 Vpp
31. Set the chip to fluorescence imaging so you can see the push off of the particles.
32. Quickly turn the signal generator Output on and off as fast as possible. The chip should create bubbles over the electrodes and particles should be released. You can do this 3 times.

### **Sample Recovery**

33. Remove the DEP setup from the microscope and take over to the lab bench.
34. Use the 1ml pipette to remove the fluid sample that is on the chip.
  - a. Gently use the pipette to move the fluid in and out of the chip several times to wash as much as possible. Collect and save this sample
  - b. Label samples as "First Wash".
35. Then use  $\sim 40 \mu\text{L}$  of TE and wash the chip again to remove the last remaining sample
  - a. Label it as "Second TE Wash".
36. Both the first and second washes should then be placed in the freezer.
37. Save the collected images to the computer hard drive using a descriptive file name

### **System Shutdown**

38. Turn off the computer
39. Turn off the syringe pump
40. Turn off the signal generator
41. Turn off the Fluorescent light source
42. The used chip needs to be
  - a. Placed back in its original plastic bag
  - b. The bag needs to be labeled with "Biohazard"
  - c. Place the bag in the used chip drawer
43. The 1 mL syringe in the hydraulic system needs to be bleached with 10% bleach

# MRMC/UCSD Rapid Isolation and Detection for RNA Biomarkers for TBI

## Annual Technical Report (Redacted Version)

Current Quarter Technical Report embedded in Annual Report

Subaward Number: 56441140

US Army MRMC Prime Award Number: W81XWH-14-2-0192

Issued 10/12/2015

Annual Technical Report Covering the Period 04/01/2105 – 09/30/2015

## 1. CURRENT QUARTER TECHNICAL REPORT 07/01/15 – 09/30/15

(Current Quarter Technical Report is redacted due to potential export control and patentability.  
Full report provided directly from Raytheon to Army.)

An underlying premise of the instant program (Rapid Isolation and Detection for RNA Biomarkers for TBI Diagnostics) is that certain variants of RNA and DNA can be sensitive and specific markers for TBI. Customarily, the TBI community invokes the Receiver Operating Characteristic (ROC) curve as the mechanism for quantifying sensitivity and selectivity, and therefore, the efficacy of a given nucleic acid variant as a discriminating marker for TBI. However, a frequent constraint is that the quantity of RNA and/or DNA is far below the limit of detection for most sensors of choice, e.g., fluorescence. Therefore, the scarce amount of RNA/DNA sample is amplified by use of the Polymerase Chain Reaction (PCR). But while PCR amplifies the original amount of RNA/DNA, PCR does not reveal how much of the original RNA/DNA was present before amplification. Therefore, most workers resort to choosing the threshold crossover cycle ( $C_T$ ) as a surrogate measure of the RNA/DNA originally in the sample. The issue with using  $C_T$  in the calculation of ROC curves is that  $C_T$  is a logarithmic representation. The quantity of RNA/DNA doubles with each PCR cycle, yielding exponential growth. Another issue is that the cycles are discrete rather than continuous. Yet, historically, the ROC was derived by radar engineers using [nearly] continuous, linear data. Therefore, the insertion of discrete, exponential PCR cycle data into the construction of ROC curves gives rise to the following key question.

*Does the insertion of PCR cycle data into ROC curve calculation compromise the ROC curve as a metric for the efficacy of specific nucleic acids as markers for TBI?*

In this annual report, we provide an analysis of “Exponential Quantization Effects on Decision Thresholds” in the context of ROC curve calculation. In this analysis, the terms, “normal” and “abnormal,” appear frequently. “Normal” relates to the probability of false alarm; “abnormal” relates to the probability of detection. These terms, and examples of their respective probability distributions, can be found in our report from the previous quarter, where we discussed the foundational underpinnings of the ROC curve and how it is derived.

At its present level, our analysis of Exponential Quantization Effects is a work-in-progress. Results obtained to date offer insights into the implications associated with Decision Thresholds for TBI in published ROC curves that have been calculated from PCR cycle data. In the coming quarter, we will confirm whether methods employed by published authors mitigate the issues that derive from discrete, exponential PCR cycle data in ROC curve calculation.

To the extent that our Exponential Quantization Effects analysis reveals implications for radar and sonar processing based on log amp detectors, the material may, potentially, be export

controlled. It may also become part of Raytheon's algorithm for predicting patient outcome, in which case, it may be patentable. (No patent has been filed as of this writing.) For these reasons, a redacted version of the report is presented here. The full analysis, formatted as a paper, is provided directly from Raytheon to the Army. (No paper has been published as of this writing.)

To highlight the features of the analysis, the Introduction section is reproduced here.

For a half century, radar and sonar digital signal processing engineers have known how to account for effects of digitization of signals by an Analog-to-Digital Converter (ADC). See, for example, Skolnik, pp. 119-125. In the early days, the ADCs had fewer bits per sample than today's devices, and the effects of quantization were relatively more severe. Over this time, our experience has been only with ADCs that sample with uniform steps sizes, and with modern resolution the quantization effects are almost negligible.

Now, we have been motivated to investigate the quantization effects of non-uniform, in fact exponential, discretization. In some common radars, this could be a model for digital thresholding after a log-amp detector when trying to measure a target's Radar Cross Section. Our motivation comes from a different domain in which diagnostic decisions are to be made based on the quantity of certain chemicals, especially RNA molecules, in blood samples. The non-linear quantization effects occur in the measurement systems that perform Polymerase Chain Reactions (PCR) to amplify the amount of these target molecules so that they may be detected.

In this paper, we indicate

- The difficulty in ROC-based decisions of exponentially quantized measurements
- The need for interpolation of exponentially quantized measurements
- The areas of concern when using mathematically ideal models for interpolating exponentially quantized measurements of random variables

Simple examples are provided using Gaussian distributions to illustrate the points.

## 2. COPY OF PRIOR QUARTER REPORT 04/01/15 – 06/30/15

(It is reasonable to concatenate the Current and Prior Quarter Reports because one flows into the other without repetition of content.)

### Table of Contents:

<b>2.1. Introduction.....</b>	<b>2-2-1</b>
2.1.1 Probability Distribution and Density Functions.....	2-2-1
2.1.2 Receiver Operating Characteristics.....	2-2-3
2.1.2.1 Theoretical Framework for ROCs.....	2-2-3
2.1.2.2 Framework for ROCs based on Unmodeled Data .....	2-2-5
2.1.3 Commentary.....	2-2-5
<b>2.2. APPLICABLE DOCUMENTS.....</b>	<b>2-2-5</b>
2.2.1 Background .....	2-2-5
2.2.2 Research.....	2-2-6
<b>2.3. Notation and Terminology for Multivariate Analysis.....</b>	<b>2-2-7</b>
2.3.1 Descriptive Statistics.....	2-2-7
2.3.2 Scaling and Mahalanobis Transformations.....	2-2-8
2.3.3 Q- and R-Techniques .....	2-2-9
<b>2.4. Methods .....</b>	<b>2-2-9</b>
2.4.1 Review of Sharm [Sha-1], et al.....	2-2-10
2.4.2 Review of Frøst [Fro-1], et al.....	2-2-12
2.4.3 Post-Hoc Testing.....	2-2-10
2.4.4 Review of Papa [Pap-1], et al.....	2-2-10
2.4.5 Review of Popper [Pop-1], et al.....	2-2-11
2.4.6 Review of Tang [Tan-1], et al.....	2-2-11
2.4.7 Review of Umali [Uma-1], et al.....	2-2-12
<b>2.5. Acronyms and Appendices.....</b>	<b>2-2-12</b>
2.5.1 List of Acronyms .....	2-2-12
2.5.2 MATLAB Code for Descriptive Statistics of MultiVariate Data .....	2-2-13

**List of Tables:**

Table 1. Common Densities Related to the Standard Normal .....2-2-2

**List of Figures:**

Figure 1. Standard Normal Density .....2-2-2  
Figure 2. Thresholding Normal Densities.....2-2-3  
Figure 3. ROC.....2-2-3  
Figure 4. ROC Generated by Small Data Sets with Area Under the ROC = 0.84.....2-2-5  
Figure 5. Histogram after Mahalanobis Transformation .....2-2-9

## 2.1 Introduction

This report presents a summary of mathematical decision methods applied to the determination and diagnosis of Traumatic Brain Injury (TBI) based on nucleic acid markers. The papers we have included are listed in paragraph 2.2.2. Many of the basic mathematical concepts and notation are available on the internet; some recommended texts are listed in our paragraph 2.2.1.

Raytheon has a great depth of background in statistical decision making derived from decades of experience in the design, development, and deployment of diverse sensor systems, such as radar and sonar. But this experience has been applied only rarely, if at all, toward bio-medical pursuits. Therefore, this study was undertaken to observe how the TBI community approaches statistical decision making. We found that, for TBI research on nucleic acids, the “ROC”, or Receiver Operating Characteristic, is the predominant tool in both sensor system design and decision making. Accordingly, this report will discuss the foundations of the ROC curve, and then move on to a brief commentary on each of the published papers that address statistical decision making based on nucleic acid markers for TBI (plus a few examples from cognate fields). We also introduce some notation for discussing the ROC.

In the present program, to be consistent with the TBI community, Raytheon expects to invoke the ROC for proof-of-principle. Thereafter, for more comprehensive and longer term predictions of patient outcome, we anticipate that our work in decision making will evolve toward multivariate analysis. For that reason, after some preliminaries to establish notation, we summarize some relevant material from the book by Mardia, *et al.* [Mar-1].

### 2.1.1 Probability Distribution and Density Functions

It is quite customary to denote by a capital letter, such as  $X$ ,  $Y$  or  $Z$ , any quantity that will result from a measurement whose value is likely to vary unpredictably, i.e., randomly. While the value of  $X$  is unpredictable, it can happen that the probability of finding the measured value in some interval is predictable and is in accordance with some “law” or model given by a function:

$$F(x) = P[X \leq x] = \text{the probability that } X \text{ will be no larger than } x,$$

called the Probability Distribution Function (PDF). If  $F(x)$  is differentiable, its derivative is denoted by  $f(x)$ , and the probabilities for finding  $X$  in some interval  $[a, b)$  is given by an integral:

$$P[a \leq X < b] = \int_a^b f(x)dx = F(b) - F(a)$$

where the last part of the equation is the Fundamental Theorem of Calculus. The function  $f(x)$  is called the probability density function (pdf), or simply the density of  $X$ .

In designing receivers, for example in radio, television, radar or sonar, there is a fundamental randomness in signal levels created by thermal noise that effects the detection of objects or signals. That randomness obeys a normal law, also called a Gaussian distribution. The standard normal density gives probabilities for a random variable  $Z$  by the integrals:

$$P[a < Z \leq b] = \int_a^b \frac{1}{\sqrt{2\pi}} e^{-\frac{x^2}{2}} dx = \frac{1}{2} \left( \operatorname{erf}\left(\frac{b}{\sqrt{2}}\right) - \operatorname{erf}\left(\frac{a}{\sqrt{2}}\right) \right)$$

The so-called error function, erf(x), is built into standard mathematics software today. The standard normal density is the familiar “bell curve” of Figure 1.

Performing mathematical operations on random variables leads to corresponding changes in the PDFs. The correspondence is explained in any probability text such as the one we reference by William Feller [Fel-1]. It is worth noting three general PDFs that easily derive from the standard normal. These three important laws, the Normal, Rayleigh, and Exponential, are summarized in Table 1.

Note that both the Rayleigh and the Exponential densities are for computing probabilities for random variables that are always positive. Hence, those densities should be treated as being 0 for negative values of x. The subscripts used in the operation creating the Rayleigh density indicates that the two standard normal random variables are independent yet obey the same probability law. Such would be the case when sampling a receiver’s noise at different times.

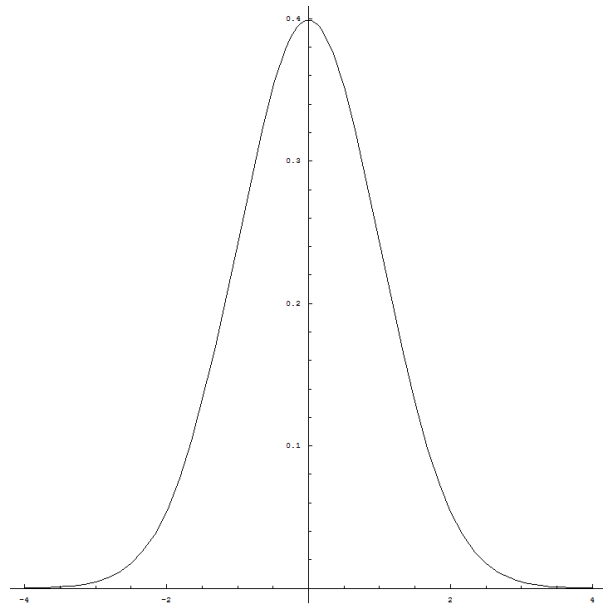


Figure 1. Standard Normal Density

Table 1. Common Densities Related to the Standard Normal

Operation	Density Formula	Name
$X = \mu + \sigma Z$	$\frac{1}{\sigma\sqrt{2\pi}} e^{-\frac{(x-\mu)^2}{2\sigma^2}}$	(General) Normal
$X = \sigma\sqrt{Z_1^2 + Z_2^2}$	$\frac{x}{\sigma^2} e^{-\frac{x^2}{2\sigma^2}}$ , and $x \geq 0$	Rayleigh
$X = \sigma^2 Z^2$	$\frac{1}{\sigma^2} e^{-\frac{x}{2\sigma^2}}$ , and $x \geq 0$	Exponential

### 2.1.2 Receiver Operating Characteristics

The ROC is a curve to aid in decision making. In classic radar engineering, the decision to analyze is whether or not to declare an aircraft to be in the field of view of the system. The stochastic nature of the decision stems from the desire to detect the aircraft at the longest range possible, where the radar signal echoed back to the receiver is very weak and on the order of magnitude of the receiver’s thermal noise. In summary, the problem is to evaluate probabilities for 2 events based on the receiver’s threshold level (assumed adjustable during design or during operation).

#### 2.1.2.1 Theoretical Framework for ROCs

In this framework, it is assumed that two (conditional) probability distribution functions model the randomness well. The first is the PDF for receiver output conditioned on there being no aircraft in the field of view. This is  $F_1(x)$ , and it is the PDF for thermal noise. In classic receivers, the normal distribution with  $\mu = 0$  and  $\sigma > 0$  is known to be an excellent fit. The parameter,  $\sigma$ , can be measured once the receiver is built, but in design it is often specified as  $\sigma^2$  in power units (power spectral density in Watts) by means of various physical (Boltzmann’s constant, temperature) and design (bandwidth, noise figure) parameters. The second required PDF is the one conditioned on there being a radar echo in the signal. In a mathematically convenient condition, the aircraft’s echo is a non-random constant value and the receiver noise simply adds to that constant level. Hence,  $F_2(x)$  is another normal distribution with a non-zero parameter  $\mu$  (mean or expected value) and the same  $\sigma$  (standard deviation) as for noise alone. The situation is summarized in Figure 2 .

Each choice of a threshold level,  $T$ , results in 2 probabilities of interest, the probability of detection

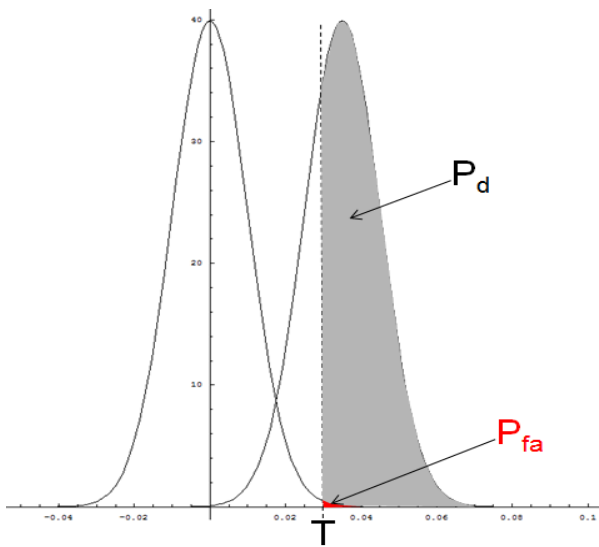


**Figure 2. Thresholding Normal Densities**  
 ( $P_d$ ) and the probability of false alarm ( $P_{fa}$ ). These probabilities are computed from the specified PDFs by integration:

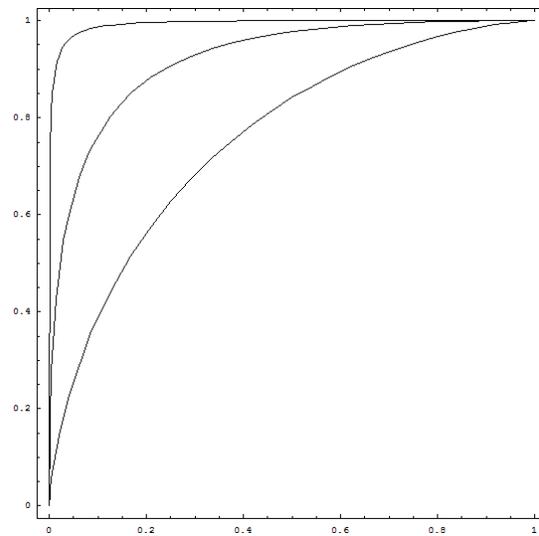


**Figure 3. ROC**

$$P_d = \int_T^{\infty} \frac{1}{\sigma \sqrt{2\pi}} e^{-\frac{(x-\mu)^2}{2\sigma^2}} dx = \frac{1}{2} \left( 1 - \operatorname{erf} \left( \frac{T - \mu}{\sigma \sqrt{2}} \right) \right)$$

$$P_{fa} = \int_T^{\infty} \frac{1}{\sigma \sqrt{2\pi}} e^{-\frac{x^2}{2\sigma^2}} dx = \frac{1}{2} \left( 1 - \operatorname{erf} \left( \frac{T}{\sigma \sqrt{2}} \right) \right)$$

Both probabilities have been written as functions of the threshold. Since the threshold is really an intermediate step in determining the value of  $P_d$  from  $P_{fa}$ , the ROC is used to write  $P_d$  as a function of  $P_{fa}$  directly by inverting the equation for  $P_{fa}$  and substituting into the equation for  $P_d$ :

$$T = \sigma \sqrt{2} \operatorname{erf}^{-1}(1 - 2P_{fa})$$

$$ROC: P_d(P_{fa}) = \frac{1}{2} \left( 1 - \operatorname{erf} \left( \operatorname{erf}^{-1}(1 - 2P_{fa}) - \frac{\mu}{\sigma \sqrt{2}} \right) \right) = 1 - F_2 \left( F_1^{-1}(1 - P_{fa}) \right)$$

The graphs of three  $P_d$  as functions of  $P_{fa}$  are depicted in Figure 3. As the aircraft signal level,  $\mu$ , is increased, the ROC curve moves deeper into the upper left-hand corner indicating that with stronger signal return, detection becomes more certain with very low false alarm rates. A convenient measure of this certainty in decision making is the area, usually between 0.5 and 1.0, under the ROC curve. As in all cases, the ROC extends from (0, 0) implying that there will be no detection when there is no probability of false alarms. It extends to (1, 1) thereby saying that detection is certain only when the false alarm rate is 100%.

### 2.1.2.2 Framework for ROCs based on Unmodeled Data

When mathematical functions for the PDFs are not established, ROCs can be generated based on 1-dimensional numerical data. The data has to be sorted into two, mutually exclusive agreed upon clusters, type 1 and type 2. The ROC gives the percentage,  $P_d$ , of type 2 data that exceed a threshold for which the percentage of type 1 data that exceed this threshold is less than or equal to the variable  $P_{fa}$ . Due to the finite size of the data matrix, the data will generate a ROC with flat intervals, a step function. The area under the curve is a natural sum of areas of rectangles corresponding to the steps. See Figure 4.

When there is a lot of data, it makes sense to approximate the data ROC with a theoretical ROC by modeling the data histograms with mathematical functions. When there is a parameterized family of PDFs that can be justified as theoretical plausible as the underlying population distribution, the decision problem reduces to parameter estimation.

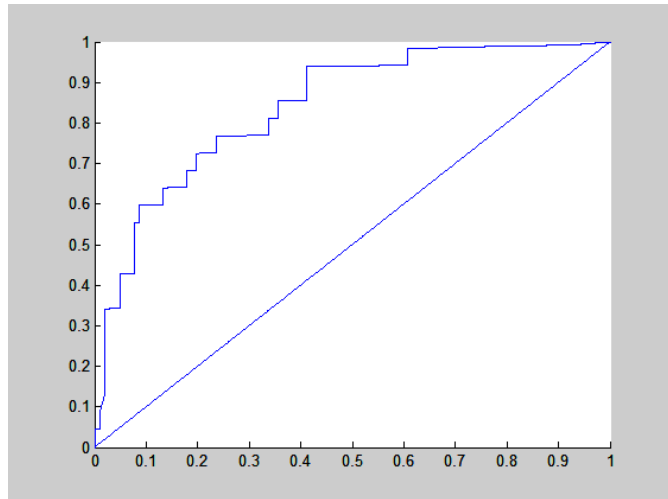


**Figure 4. ROC Generated by Small Data Sets with Area Under the ROC = 0.84**

### 2.1.3 Commentary

It is perhaps worth stressing that the data available today to the receiver design engineer is voluminous and inexpensive. The normal distribution is an excellent model verified by mathematical theory, experimentation, and theoretical Physics.

A radar operator sets a threshold for a very low false alarm rate, and the performance of the system is predicted well by the ROC. In biomedical stochastic decision making, the data may be scarce and expensive to obtain. There can be much greater uncertainty in the goodness of the modeling law for values far from the mean value, the so-called tails of the distribution. In radar operations, there is a corresponding disappointment in system performance when the background interference is not due to thermal noise but, say, to precipitation or sea surface clutter whose distribution can be a far cry from normal. The system designer is always looking for decision criteria that are

- Optimal – make the best use of the expensive data available
- Robust – make good decisions even when the stochastic models are not well known
- Extensible – make better decisions whenever more data, or a different sort, is available

## 2.2 APPLICABLE DOCUMENTS

### 2.2.1 Background

[Fel-1] Feller, William, *An Introduction to Probability Theory and Its Applications*, vol I and II, John Wiley & Sons, NY, 1971

[Hog-1] Hogg, Robert V. and Craig, Allen, T., *Introduction to Mathematical Statistics*, 4<sup>th</sup> Ed, Macmillan Pub Co, NY, 1978

[Mar-1] Mardia, K. V., Kent, J. T., and Bibby, J. M., *Multivariate Analysis*, Academic Press, NY, 1979.

### 2.2.2 Research

[Gov-1] Govindarajulu, Z. and Leslie, R.T., Annotated Bibliography on Robustness Studies of Statistical Procedures, DHEW Pub No. HSM 72-1051, US Dept Health, Education and Welfare, National Center for Health Statistics, Rockville, MD, April 1972

[Las-1] Lasko, T. A., Bhaqwat, J.G., Zou, K.H., and Ohno-Machado, L., The use of receiver operating characteristic curves in biomedical infomatics, *J. of Biomedical Infomatics*, 38: 404-415, 2005.

[Pap-1] Papa, Linda, Lewis, Lawrence M., Falk, Jay L., Zhang, Zhiquan, Silvestri, Salvatore, Giordano, Philip, Brophy, Gretchen M., Demery, Jason A., Dixit, Neha K., Ferguson, Ian, Liu, Ming Cheng, Mo, Jixiang, Akinyi, Linnet, Schmid, Kara, Mondello, Stefania, Robertson, Claudia S., Tortella, Frank C., Hayes, Ronald L., Wang, Kevin K. W., Elevated levels of serum glial fibrillary acidic protein breakdown products in mild and moderate traumatic brain injury are associated with intracranial lesions and neurosurgical intervention, *Annals of Emergency Medicine*, 59 No. 6, (471-483), June 2012.

[Pap-2] Papa, Linda, Lewis, Lawrence M., Silvestri, Salvatore, Falk, Jay L., Giordano, Philip, Brophy, Gretchen M., Demery, Jason A., Ming Cheng, Mo, Jixiang, Akinyi, Linnet, Mondello, Stefania, Schmid, Kara, Robertson, Claudia S., Tortella, Frank C., Hayes, Ronald L., Wang, Kevin K. W., Serum levels of ubiquitin C-terminal hydrolase distinguish mild traumatic brain injury from trauma controls and are elevated in mild and moderate traumatic brain injury patients with intracranial lesions and neurosurgical intervention, *J. Trauma*, 72 No. 5, (1335-1344), 2012.

[Pap-3] Papa, Linda, Linnet, Akinyi, Liu, Ming Chen, Pineda, Jose A., Tepas III, Joseph J., Oli, Monika W., Zheng, Wenrong, Robinson, Gillian, Robicsek, Steven A., Gabrielli, Andrea, Heaton, Shelley C., Hannay, Julia, Demery, Jason A. Brophy, Gretchen M., Layon, Joe, Robertson, Claudia S., Hayes, Ronald L., and Wang, Kevin K. W., Ubiquitin C-terminal hydrolase is a novel biomarker in humans for severe traumatic brain injury, *Crit Care Med*, 38, No. 1, 138- 144, 2010.

[Pop-1] Popper, Richard and Heymann, Hildegard, Analyzing differences among products and panelists by multidimensional scaling, *Multivariate of Data in Sensory Science*, 159-184, 1996.

[Red-1] Redell, John B., Moore, Anthony N., Ward, III, Norman H., Hergenroeder, Georgene W., and Dash, Pramod K., Human traumatic brain injury alters plasma microRNA levels”, *J. of Neurotrauma*, 27:2147-2156, 2010.

[Sha-1] Sharma, Anuj, Raghavendar, Chandran, Barry, Erin S., Bhomia, Manish, Hutchinson, Mary Anne, Balakathiresan, Nagaraja S., Grunberg, Neil E., and Maheshwari, Radha, K., Identification of serum microRNA signature for diagnosis of mild traumatic brain injury in a closed head injury model, *PLoS ONE* 9(11): e112019, doi: 10.1371/journal.pone.0112019, November 7, 2014.

[Tan-1] Tang, Chen, Heymann, Hildegard, and Hsieh, Fu-hung, Alternatives to data averaging of consumer preference data, *Food and Quality Preference*, **11**, 94-104, 2000.

[Uma-1] Umali, Alona P., Ghanem, Eman, Hopfer, Helene, Hussain, Ahmed, Kao, Yu-ting, Zabanal, Lianna G., Wilkins, Brandon J., Hobza, Courtney, Quach, Duan K., Morgan Fredell, Heymann, Hildegard, Anslyn, Eric V., Grape and wine sensory attributes correlate with pattern-based discrimination of Cabernet Sauvignon wines by a peptidic sensor array, *Tetrahedron*, **71**, No. 20, (20 May 2015) 3095-3099. <http://dx.doi.org/10.1016/j.tet.2014.09.062>

[Fro-1] Frøst, Michael Bom, Heymann, Hildegard, Bredie, Wender L.P., Dijksterhuis, Garnt B., Martens, Magni, Sensory measurement of dynamic flavour intensity in ice cream with different fat levels and flavourings, *Food Quality and Preference*, **16** (2005) 305–314.

## 2.3 Notation and terminology for Multivariate Analysis

Here we provide a summary of notation and terminology commonly used in multivariate statistics such as presented in the book by Mardia, *et al.* [Mar-1]. The convenient notation uses linear algebra, matrices and vectors. A data matrix,  $\mathbf{X}$ , is established with columns corresponding to measurements (test results) from some number  $M$  of tests to be run. Each row of  $\mathbf{X}$  corresponds to a different subject (patient), and the total number of rows will be denoted by  $N$ . A database of additional data may be appended to  $\mathbf{X}$ , potentially including some kind of index code (as an anonymous alternative to the patient's name), age, gender, etc. Such auxiliary data can be useful in forming subgroups of the test results, but initially we focus on  $\mathbf{X}$  in its entirety.

### 2.3.1 Descriptive Statistics

The first descriptive statistic is the **mean vector** whose components are the averages of the  $M$  tests over the  $N$  subjects. The linear algebra notation for finding the mean vector uses a vector (matrix),  $\mathbf{1}$ , with  $N$  rows and 1 column and all entries equal to 1. Then, the mean vector can be computed as  $(1/N) \mathbf{X}^T \mathbf{1}$ , where the superscript “T” means the prior matrix is to be transposed. Typographically, this is much more compact than the usual notation,

$$\bar{x} = \begin{bmatrix} \bar{x}_1 \\ \vdots \\ \bar{x}_M \end{bmatrix} = \begin{bmatrix} \frac{1}{N} \sum_{n=1}^N x_{n1} \\ \vdots \\ \frac{1}{N} \sum_{n=1}^N x_{nM} \end{bmatrix}.$$

Also, and not insignificantly, this matrix notation facilitates very efficient analysis tools in mathematical packages such as MATLAB®.

The sample **covariance matrix**,  $S$ , is computed in matrix notation using the  $N \times N$  “centering matrix”,  $H = I - (1/N)\mathbf{1}\mathbf{1}^T$ . Using  $H$ , the sample covariance matrix is  $S = (1/N)\mathbf{X}^T\mathbf{H}\mathbf{X}$ . The  $S$  matrix is an  $M \times M$  matrix, and since generally  $M$  is much smaller than  $N$ ,  $S$  represents a great reduction in the dimensions of data to be analyzed. The sample correlation matrix,  $R$ , is computed with the help of another matrix,  $D$ .  $D$  is a diagonal  $M \times M$  matrix whose diagonal entries are the square roots of the diagonal entries of  $S$ , i.e. the sample standard deviations. Then,  $R = D^{-1}SD^{-1}$ , where the superscript “-1” means matrix inverse. If  $R$  equals the  $M \times M$  identity matrix, then the data is said to be statistically uncorrelated.

Two scalar-valued statistics that mirror the one-dimensional variance of data are the **generalized variance**,  $|S|$  = the determinant of the sample covariance matrix, and the **total variation**,  $\text{tr}(S)$  = the trace of the sample covariance matrix. Both of these values are generally painful to compute by hand, but trivial to evaluate in MATLAB once the data matrix is established in the tool.

### 2.3.2 Scaling and Mahalanobis Transformations

A common way to deal with multivariate problems is to look for ways to reduce the dimensionality and use one-dimensional decision strategies. Linear combinations of the test data are a basic tool for this reduction. The notation for this analysis is again from linear algebra. Consider any  $M$  dimensional vector,  $\mathbf{a} = \langle a_1, \dots, a_M \rangle$ , of fixed scalar values. For the  $r^{\text{th}}$  patient, whose test results are  $\langle x_{r1}, \dots, x_{rM} \rangle$  form the 1-dimensional statistic  $y_r$  by means of the dot (inner) product of  $\mathbf{a}$  with  $\mathbf{x}_r = \langle x_{r1}, \dots, x_{rM} \rangle$ :  $y_r = a_1 x_{r1} + \dots + a_M x_{rM}$ . A vector,  $\mathbf{y}$ , results from scaling each patient’s test scores by the dot product with  $\mathbf{a}$ . The mean or average of the scaled combinations of the test results is the dot product of  $\mathbf{a}$  with the mean vector:

$$\bar{y} = \mathbf{a}^T \bar{\mathbf{x}} = \mathbf{a} \cdot \bar{\mathbf{x}}.$$

There is a scaling that normalizes the test data to have means equal to zero and variances equal to 1. The covariance matrix after normalization is just the correlation matrix,  $R$ , of the original data. In matrix notation, normalization of the  $r^{\text{th}}$  patient’s results is given by

$$y_r = D^{-1}(\mathbf{x}_r - \bar{\mathbf{x}}),$$

where  $D$  is the diagonal matrix already introduced.

In linear algebra, it is commonly taught how to transform a spanning set of vectors into an orthonormal set of vectors. The same processes can be applied to vectors of data to produce uncorrelated scaled data that are uncorrelated (orthogonal). Applying this transformation in matrix notation is called the Mahalanobis transformation. The matrix involved in this transformation is the inverse of the Cholesky Square Root,  $S^{-1/2}$ , of the covariance matrix,  $S$ . With the MATLAB tool, it is easy to compute the Mahalanobis transformation:

$$\mathbf{z}_r = S^{-1/2}(\mathbf{x}_r - \bar{\mathbf{x}}).$$

The covariance matrix of this transformed data matrix,  $\mathbf{Z}$ , is the  $N \times N$  identity matrix,  $\mathbf{I}$ .

We used MATLAB to generate random data sets and perform the Mahalanobis transformation. We then created histograms of  $\mathbf{Z}$  and plotted them against a standard normal distribution. A typical result is depicted in Figure 5. The colors in the histogram represent the scaled test scores from 200 subjects. If the underlying data is highly skewed, it may take a lot of subjects before the Mahalanobis histogram matches the normal density well, but it is reasonable, by virtue of the Central Limit Theorem, to expect a close match for large data sets. The MATLAB code for this figure is included in an appendix to this paper.

### 2.3.3 Q- and R-Techniques

When comparing the “variables” or test scores (the columns of the data matrix), the correlation matrix,  $\mathbf{R}$ , plays a major role. So, statistical strategies for analysis of the variables are referred to as R-techniques. When comparing the rows, i.e., the subjects or patients, the statistical strategies are called Q-techniques. The Mahalanobis Distance,  $D_{ij}$ , between 2 rows of the data matrix,  $\mathbf{X}$ , is computed by the formula,

$$D_{ij}^2 = (\mathbf{x}_i - \mathbf{x}_j)^T \mathbf{S}^{-1} (\mathbf{x}_i - \mathbf{x}_j).$$

The Mahalanobis distance underlies Hotelling’s  $T^2$  test and the theory of discriminant analysis, a Q-technique.

MATLAB includes a built-in function to compute the Mahalanobis distance of rows of a data matrix,  $\mathbf{Y}$ , from mean of another data matrix,  $\mathbf{X}$ . Note that  $\mathbf{Y}$  can equal  $\mathbf{X}$ .

### 2.4 Methods Used

The primary goal of this literature summary is to summarize statistical techniques and software packages commonly used. A goal will be to focus on an application to measurements of circulating microRNAs (miRNAs) present in the serum/plasma characteristically altered by traumatic brain injury (TBI). Plasma-derived miRNA biomarkers, used in combination with established clinical practices such as imaging, neurocognitive and motor examinations, have the potential to improve TBI patient classification and possibly management [Red-1]. Statistical techniques include basic descriptive statistics and the ROC. See [Red-1] and [Las-1].

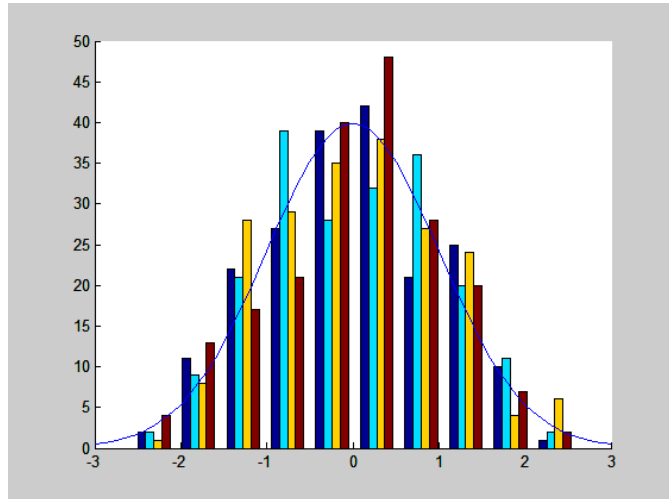


**Figure 5. Histogram after Mahalanobis Transformation**

### **2.4.1 A Biomedical Sampling of Methods Used**

A convenient starting place in researching robust statistical analysis methods used in the health sciences is the reference [Gov-1]. The roughly 360 scholarly articles highlighted in this paper are too broad to summarize. Not surprising (in light of the Central Limit Theorem) many statistical procedures are robust, in the sense of becoming insensitive to slight departures from postulated assumptions, when the sample size is sufficiently large. While we cannot recommend spending the time to master the works in the bibliography of Govindarajulu and Leslie, the introduction discussing the problems of robustness is worthwhile.

### **2.4.2 Review of Sharm [Sha-1], et al.**

In this paper, acute phase miRNA changes in the serum were measured to determine the feasibility of using miRNA as diagnostic markers of mild Traumatic Brain Injury (mTBI). The paper begins with a discussion of mTBI in accordance with the Glasgow Coma Scale (GCS). Experiments measuring ASR, NSS-R, and OFL were described. Bioinformatics analyses using the QIAGEN's Ingenuity Pathway Analysis (IPA) and DNA Intelligent Analysis (DIANA)-miRPath software showed that the number of significantly modulated serum miRNAs predicted to be involved in brain related functions increased with the severity of the injury. Measurements were analyzed using analysis of covariance (ANCOVA) and repeated measures analysis of covariance (rmANCOVA). MiRNA array threshold cycle values were imported into the Real-Time StatMiner Software V.4.5.0.7 (Integromics, Madison, WI).

In conclusion, a cohort of 13 serum miRNAs identified in this study, may be used as acute biomarkers of mTBI regardless of any neurobehavioral or cognitive alterations following the injury. Future studies will be needed to validate this cohort of 13 miRNAs as acute biomarkers of mTBI in the other animal models of injury and in the human mTBI. In addition, further behavioral studies will be needed to identify the long-term cognitive deficits and/or sleep disorders in the mTBI model described in this study. Such long-term studies will also be able to determine the prognostic value of the miRNAs identified in this study as acute biomarkers of mTBI.

### **2.4.3 Post-Hoc Testing**

[http://www.unt.edu/rss/class/Jon/ISSS\\_SC/Module009/issm\\_m91\\_onewayanova/node7.html](http://www.unt.edu/rss/class/Jon/ISSS_SC/Module009/issm_m91_onewayanova/node7.html)

### **2.4.4 Review of Papa [Pap-1], et al.**

This study examines whether serum levels of glial fibrillary acidic protein breakdown products (GFAP-BDP) are elevated in patients with mild and moderate traumatic brain injury compared with controls and whether they are associated with traumatic intracranial lesions on computed tomography (CT) scan (positive CT result) and with having a neurosurgical intervention. The data to be statistically analyzed is not multivariate.

This study enrolled adult patients presenting to 3 Level I trauma centers after blunt head trauma with loss of consciousness, amnesia, or disorientation and a Glasgow Coma Scale (GCS) score of

9 to 15. Control groups included normal uninjured controls and trauma controls presenting the emergency department with orthopedic injuries or a motor vehicle crash without traumatic brain injury. Blood samples were obtained in all patients within 4 hours of injury and measured by enzyme-linked immunosorbent assay for GFAP-BDP (nanograms/milliliter).

Of the 307 patients enrolled, 108 were patients with traumatic brain injury (97 with GCS score 13 to 15 and 11 with GCS score 9 to 12) and 199 were controls (176 normal controls and 16 motor vehicle crash controls and 7 orthopedic controls). Receiver operating characteristic curves demonstrated that early GFAP-BDP levels were able to distinguish patients with traumatic brain injury from uninjured controls with an area under the curve of 0.90 (95% confidence interval [CI] 0.86 to 0.94) and differentiated traumatic brain injury with a GCS score of 15 with an area under the curve of 0.88 (95% CI 0.82 to 0.93). Thirty-two patients with traumatic brain injury (30%) had lesions on CT. The area under these curves for discriminating patients with CT lesions versus those without CT lesions was 0.79 (95% CI 0.69 to 0.89). Moreover, the receiver operating characteristic curve for distinguishing neurosurgical intervention from no neurosurgical intervention yielded an area under the curve of 0.87 (95% CI 0.77 to 0.96). All analyses were performed with the statistical software package PASW (formally SPSS, version 17.0; IBM Corporation, Somers, NY)

GFAP-BDP is detectable in serum within an hour of injury and is associated with measures of injury severity, including the GCS score, CT lesions, and neurosurgical intervention. Further study is required to validate these findings before clinical application.

A very much related paper [Pap-2] was published in the periodical *J. Trauma* with only a slight change in the list of co-authors. The paper presents a study on 96 TBI patients and a control group of 199 looking at levels of UCH-L1 to identify patients with mild and moderate TBI. One analysis feature of note was how the authors handled values of UCH-L1 when not actually detected. They analyzed the Lower Limit Of Detection (LOD, found to be 0.030 ng/mL), and assigned a value of 0.015 ng/mL (50% of the LOD) whenever a patient's UCH-L1 level was undetected. Descriptive statistics, tests of normality, analysis of variance (ANOVA) were used as was the ROC. They used the software package PASW 17.0 by IBM.

Much of the work of this team of researchers traces to an older paper [Pap-3]. That paper used SPSS statistical software in analysis of measurements from severe TBI patients.

#### **2.4.5 Review of Popper [Pop-1], et al.**

The data analysis of Popper and Heymann was done using IBM's SPSS Statistics software and the SYSTAT software package. The primary analytic technique is Multidimensional Scaling (MDS) as described in Chapter 14 of our reference by Mardia [Mar-1].

#### **2.4.6 Review of Tang [Tan-1], et al.**

The paper [Tan-1] uses principal component analysis to analyze consumer data where the mean vector is not necessarily representative of any of the subjects. The multivariate analysis

computer software package used was SAS<sup>®</sup>. A comparison was done to evaluate the effectiveness of a variety of statistical descriptions of the measurements. In particular, a cluster analysis (see Chapter 13 of [Mar-1]) was able to discern a significant difference between Asian and non-Asian consumer preferences.

**2.4.7 Review of Umali [Uma-1], et al.**

Linear Discriminant Analysis (LDA) was used for classification of the wine samples. Partial Least Squares Regression (PLSR) was used for the correlation of wine sensory attributes to the peptide-based receptor responses. Data analysis was done using the software XLSTAT (Addinsoft, New York) and R. Absorbance values due to wine without the sensing ensembles were subtracted from the final absorbance change before the multivariate data analysis was performed.

**2.4.8 Review of Frøst [Fro-1], et al.**

Data were analysed by ANOVA, principal component analysis (PCA) and ANOVA partial least squares regression (APLSR). All uni-variate analyses were performed in SPSS (v10.0.0, SPSS Inc. Chicago, IL., USA). Unscrambler (v7.6, Camo A/S, Trondheim, Norway) was used for multivariate data analysis. For multivariate analyses cross validation was performed, leaving out one replicate at a time (cf. Martens & Næs, 1989). Jack-knifing with sensory replicates served as the validation tool for all multivariate analysis, comparing the perturbed model parameter estimates from cross-validation with the estimates for the full model (Martens & Martens, 2000).

**2.5 Acronyms and Appendices**

**2.5.1 List of Acronyms**

ASR	Acoustic Startle Response
GCS	Glasgow Coma Scale
LOD	Lower Limit Of Detection
NSS-R	Neurobehavioral Severity Scale-Revised
OFL	Open Field Locomotion
PDF	Probability Distribution Function
pdf	Probability Density Function
ROC	Receiver Operating Characteristic
UCH-L1	Ubiquitin C-terminal Hydrolase

## 2.5.2 MATLAB Code for Descriptive Statistics of MultiVariate Data

```

% Multivariate Analysis
% Copyright (C) 2015 - Raytheon Company - Integrated Defense Systems
% Author: Tom Wood
%-----
clear All; close All; format compact;
%-----
%
% Create a Data Matrix
nN = 168; mM = 4; % Warning: nN,mM < 20000 or else!
X = randn(nN,mM); % Uses no toolbox license
%X = random('rayl',2,[nN,mM]); % Uses the Statistics toolbox license
X(:,1) = (X(:,1)+ X(:,2))/2.; X(:,2) = (X(:,2)+ X(:,3))/2.;
X(:,3) = (X(:,3)+ X(:,4))/2.; X(:,4) = (X(:,4)+ X(:,1))/2.;
X(:,1) = (X(:,1)+ X(:,2))/2.; X(:,2) = (X(:,2)+ X(:,3))/2.;
X(:,3) = (X(:,3)+ X(:,4))/2.; X(:,4) = (X(:,4)+ X(:,1))/2.;
%-----
% Form Descriptive Statistics: mean vector and sample covariance matrix
%
iI = ones(nN,1);
meansV = (1/nN)*transpose(X)*iI; % Column vector of means (nM)
figure; bar(transpose(meansV));
H = eye(nN) - (1/nN)*(iI * transpose(iI)); % Centering Matrix (nN x nN)
S = (1/nN)*transpose(X)*H*X % S is pos def if nN > mM
D = sqrt(diag(diag(S)));
R = inv(D) * S * inv(D) % Sample Correlation Matrix
genVar = det(S) % Generalize Variance
totVar = trace(S) % total variation
%-----
% Perform the Mahalanobis Transformation
%
CSR = transpose(chol(S)); % Cholesky Square Root of S
CSR * transpose(CSR) - S % Check for round-off errors
A = inv(CSR); % Mahalanobis scaling
Z = X;
for r = 1:nN
    Z(r,:) = transpose(A*(transpose(Z(r,:)) - meansV));
end
meansVz = (1/nN)*transpose(Z)*iI; % meansVz are all tiny
Sz = (1/nN)*transpose(Z)*H*Z; % Sz should be close to I
genVarZ = det(Sz); % Generalize Variance ~ 1
totVarZ = trace(Sz); % total variation ~ mM
figure; hold on; hist(Z); % Histogram after Mahalanobis
t = [-4:0.1:4]; yy = (1/sqrt(2*pi()))*exp(-(t .* t)/2);
plot(t, (nN/1.4)*yy); % Compare with a Normal Density

```

```

figure; plot(sqrt(mahal(X,X))); % Mahalanobis distances (noise)
figure; glyphplot(X, 'glyph', 'face');
%-----
% ROC Developed from Small Data Sets U and V
%
kN = 107; jN = 24; NN = 999;
U = randn(kN,1); V = randn(jN,1) + 1.75; % Generate Data Sets
aa = min(min(U),min(V)); bb = max(max(U),max(V));
Pfa = [0:1/NN:1]; Pd = Pfa;
T = [aa:(bb - aa)/NN : bb]; figure; plot(T);
% Determine the Data False Alarm Rate for NN+1 Thresholds
for ii = 1:NN
    for kk = 1:kN
        if U(kk) <= T(ii)
            Pfa(ii+1) = Pfa(ii+1) + 1;
        end
    end
end
Pfa = Pfa/max(Pfa); Pfa(NN+1) = 1;
figure; hold on; plot(Pfa);
% Determine the Data Detection Rate for NN+1 Thresholds
for ii = 1:NN
    for jj = 1:jN
        if V(jj) <= T(ii)
            Pd(ii+1) = Pd(ii+1) + 1;
        end
    end
end
Pd = Pd/max(Pd); Pd(NN+1) = 1;
plot(Pd, 'r');
figure; hold on; plot([0:1/NN:1],[0:1/NN:1]); plot(1-Pfa,1-Pd);
% Determine the Area under the ROC
Area = 0;
for ii = 1:NN
    Area = Area + (1-Pd(ii+1))*(Pfa(ii+1)-Pfa(ii));
end
AreaUnderROC = Area

```

### **3.3 Opportunities for training and professional development provided by this project**

Nothing to report

### **3.4 Disseminated of results to communities of interest**

A manuscript has been prepared for ACS Nano Journal title “Recovery of Exosomes Containing Circulating Cell-Free RNA from Human Plasma Using High Conductance Dielectrophoresis”, authored by Stuart Ibsen, Jennifer Wright, Sejung Kim, Seo-Yeon Ko, Jiye Ong, Sareh Manouchehri, Johnny Akers, Clark Chen and Michael J. Heller. This paper once published should be of considerable interest for biomedical and molecular diagnostic researchers. Some project results on exosome and ccf-RNA isolation by DEP have been presented at recent technical meetings.

### **3.5 Project Goals and Objectives for next period**

#### **IRB Final Approval and TBI Samples**

Upon IRB final approval we will immediately proceed and complete 1<sup>st</sup> year goals using available TBI samples. Because of our success on the other important project goals we should be able to complete this work on initial TBI samples within 3-4 weeks of IRB final approval. We can then proceed with collecting other TBI samples as described in the SOW for year two project work. Samples will be provided by Dr. Clark Chen (UCSD Moores Cancer Center), UCSD Trauma Center, La Jolla, CA; Dr. Josh Duckworth (Department of Neurology, Uniformed Services University of the Health Sciences, Bethesda MD); and Dr. Jason Ballie, (Naval Medical Center San Diego (NMCS) Defense and Veterans Brain Injury Center (DVBIC, San Diego, CA). The primary goal is to identify specific mRNAs and miRNAs present in the TBI samples.

#### **DEP system automation**

The future plans for the development of the DEP system are to begin automating various aspects of data collection, signal generation, and chip handling to make it easier for the user to run chips, which will become very important as the number of samples increases in the next year. These automations will be done through the creation of a new LabView based user interface that will control the camera, the signal generator, and the syringe pump used to wash the samples. These changes will be accomplished in parallel with the existing system so the continuous work that is currently ongoing will not be interrupted. The changes will be phased in over the next three months.

#### **Sample processing optimization and improving RNA biomarker detection and analysis**

- Once the IRB has been approved, the clinical samples will arrive to us and we will be able to use the existing and newly improved system to collect ccf-RNA from those samples for mRNA and miRNA biomarker analysis

- Eliminate need for RNA extraction kit to lyse the exosomes and release the RNA from inside.
  - Further optimization of process for releasing ccf-RNA from the collected exosomes.
  - Optimize heating and surfactants (Tween-20, TritonX) treatments
- Design and test RT-PCR primers for other miRNA biomarkers
  - miRNA can be found in the blood/plasma/serum of healthy donors, so quantification is important. Rather than looking for whether or not a particular miRNA is present, we have to determine how the amount of miRNA present compares to that of healthy volunteers and those with non-TBI injuries.
- Continue to design and test more brain-specific mRNA biomarkers
  - Improve specificity and sensitivity of primers for some targets (GFAP)
- Continue to optimize downstream assay protocols
  - RT-PCR reaction – Thus far, we have focused on optimizing the PCR and qPCR reactions of our post-DEP assay, but we may also improve detection of transcripts of interest by improving the RT-PCR reaction. One way we can do this is to use specific primers during the RT reaction rather than random hexamers, which amplify a number of transcripts. While there are some benefits to using random hexamers during the RT-PCR step, the specific primers are more useful when we know the transcript(s) for which we are looking.
  - PCR or qPCR reactions – as we've already mentioned, PCR or qPCR reactions can be made more sensitive by redesigning primers as well as changing cycling conditions
  - An additional way to make our assays more sensitive is to combine the RT-PCR and qPCR steps. This way, all of cDNA sample that is made is used in the subsequent PCR or qPCR reaction. At this time, only a fourth or a fifth of this sample is used.
- Improve on-chip fluorescence detection techniques for exosomes, ccf-RNA, ccf-DNA and protein aggregates.
- Begin planning design and strategy for POC of DEP system, including on-chip PCR which will allow seamless sample-to-answer for TBI diagnostics and patient monitoring.

## **4. IMPACT**

### **4.1 Impact on the development of the principal discipline(s) of the project**

We believe that the results of our first year project work will have a significant impact on TBI diagnostics and patient monitoring. We have demonstrated that we can use DEP to rapidly isolate brain-related exosomes and ccf-RNA from plasma and then identify specific mRNAs. As stated previously, while RNA biomarkers are becoming more important for TBI diagnostics, present methods, which are time consuming and complex, greatly limit their applicability.

### **4.2 Impact on other disciplines**

The results of first year project work on demonstrating rapid DEP isolation of brain-related exosomes and ccf-RNA from plasma will impact other related areas such as Alzheimer's disease and sports injury. It will also have a significant impact on cancer diagnostics, where isolation of exosomes and RNA detection is very important for enabling future "liquid biopsy" molecular diagnostics.

#### **4.3 Impact on technology transfer**

The results of first year project work on demonstrating rapid DEP isolation of brain-related exosomes and ccf-RNA from plasma will have impact on technology transfer as it demonstrates overall viability of the DEP technology for a wide variety of diagnostic applications. At this time a new company, Biological Dynamics (San Diego, CA), is in the process of commercializing DEP microarray devices and systems for cancer diagnostics. This is the DEP technology originally developed in the Heller lab and licensed from UCSD by Biological Dynamics. Additionally, along with Raytheon (Project CoPI), we will be evaluating future POC and field packaging for DEP-based diagnostic systems.

#### **4.4 Impact on society beyond science and technology**

TBI can lead to other neurodegenerative processes that directly decrease quality of life and have a major impact on the patient's long-term psychological health. This has significant negative effects on family members and is costly to society in general. We believe new TBI molecular diagnostics for patient monitoring and management could identify patients that have had a TBI event allowing earlier medical and therapeutic intervention. This can catch and address complications earlier thereby ameliorating short term and long term patient health problems and ultimately reduce resulting negative effects on family members and society in general.

### **5. CHANGES/PROBLEMS**

#### **5.1 Changes in approach and reasons for change**

Because we were waiting on final approval of our IRB by HRPO (ORP/USAMRMC), we were not able to proceed on project efforts and goals related to using and obtaining TBI patient samples. During that time we placed more efforts on further development and optimization of the DEP technology for better isolation, detection and analysis of RNA using the glioblastoma model. While a delay, this does not deviate from our basic project plan.

#### **5.2 Actual or anticipated problems or delays and actions or plans to resolve them**

Again, while waiting on final approval of our IRB by HRPO (ORP/USAMRMC) has delayed project efforts related to using and obtaining TBI patient samples, we are ready to immediately proceed and complete 1<sup>st</sup> year project goals in this area. We should be able to complete this work

on initial TBI samples within 3-4 weeks of IRB final approval. We can then proceed with collecting other TBI samples as described in the SOW for year two project work.

### **5.3 Changes that had a significant impact on expenditures**

None at this time

### **5.4 Significant changes in use or care of human subjects, vertebrate animals, biohazards, and/or select agents**

Not applicable

### **5.5 Significant changes in use or care of human subjects**

Not applicable

### **5.6 Significant changes in use or care of vertebrate animals.**

Not applicable

### **5.7 Significant changes in use of biohazards and/or select agents**

Not applicable

## **6. PRODUCTS**

### **Publications, conference papers, and presentations**

#### **Journal publications.**

A manuscript (attached in the Appendix) has been prepared for ACS Nano Journal title “Recovery of Exosomes Containing Circulating Cell-Free RNA from Human Plasma Using High Conductance Dielectrophoresis”, authored by Stuart Ibsen, Jennifer Wright, Sejung Kim, Seo-Yeon Ko, Jiye Ong, Sareh Manouchehri, Johnny Akers, Clark Chen and Michael J. Heller.

#### **Books or other non-periodical, one-time publications.**

Nothing to report

#### **Other publications, conference papers, and presentations.**

Some project results on exosome and ccf-RNA isolation by DEP have been presented at recent technical meetings, these included: **Fusion Conference Limited, Personalized Medicine,**

Tucson, AZ, Sept. 30 , 2015; **SelectBio Conference NGS, SCA, MS & The Road to Diagnostics**, Del Mar, CA, Sept. 29, 2015; **San Diego BRAIN Consortium Symposium: Neurotechnology Research in San Diego** , La Jolla, CA, Sept. 19, 2015; **CNAPS 2015**, Berlin, Germany, Sept. 11, 2015; and **CHI Next Generation Dx Summit, C2 – Predictive Cancer Biomarkers** , Washington DC, August 18, 2015

**Website(s) or other Internet site(s)**

Nothing to report

**Technologies or techniques**

New DEP MicroArray (Chip) and system protocols were described in the above Accomplishments section of the report.

**Inventions, patent applications, and/or licenses**

An invention disclosure titled “Electrokinetic Devices and Methods for Sample to Answer Molecular Diagnostics for Exosomes, RNA, DNA, Protein and other Biomarkers“ will be sent under separate cover to our Science Officer, Dr. Anthony Pacifico, and our Neurotrauma Research Portfolio Manager, Dr. Alicia Tamara Crowder (U.S. Army Medical Research and Materiel Command Combat Casualty Care Research Program).

**Other Products**

Nothing to report

**7. PARTICIPANTS & OTHER COLLABORTING ORGANIZATIONS**

- **Individuals that worked on the project**

<b>Personnel</b>	<b>Role</b>	<b>Percent Effort</b>
Dr. Michael J. Heller	Project PI – Provide overall management and direction for the TBI project.	0.25 cal mos

Dr. Clark Chen	Project Co-PI – Prepare project IRB and provide TBI samples. Provide expertise on brain-related RNA.	0.25 cal mos
Dr. Stuart Ibsen	Postdoc - Main role is to run and maintain the HC-DEP devices and systems, and continue to develop it for our specific experimental needs. This includes optimizing the technology for highest RNA collection efficiency and elution.	100%/12 cal mos
Dr. Jennifer (Marciniak) Wright	Post doc – Main role is to develop RT-PCR primers and protocols for testing collected RNA from blood, plasma, and other samples.	100%/12 cal mos
Tsukasa Takahashi	Graduate student researcher/Staff Research Associate – helped obtain supplies necessary for this project, as well as making necessary components for the HC- DEP system. (1 <sup>st</sup> , 2 <sup>nd</sup> , and part of 3 <sup>rd</sup> quarter project involvement)	34%/3 cal mos
August Modestino Silva	Graduate student researcher – Start-Up Oct-Nov 2014	45%/1.5 cal mos
Youngjun Song	Graduate student researcher – Start-Up Oct-Dec, 2014	50%/0.50 cal mos
Daniel Heineck	Graduate student research – DEP systems	13%/1.3 cal mos
Taeseok Oh	Graduate student researcher – Initiated work on on-chip fluorescent detection of RNA	34%/3.4 cal mos

Sejung Kim	Graduate student researcher- Carried out general work for the TBI project start-up (1 <sup>st</sup> quarter). SEM work (3 <sup>rd</sup> & 4thquarters)	23%/2.3 cal mos
Dr. James Wurzbach	Co-PI Raytheon- The UCSD- Raytheon sub-contract has been completed.	0%

- **Has there been a change in the active other support of the PD/PI(s) or senior/key personnel since the last reporting period?**

No.

- **What other organizations were involved as partners?**

Nothing to report

## **8. SPECIAL REPORTING REQUIREMENTS**

- **COLLABORATIVE AWARDS:**

Nothing to report

# Rapid Isolation and Detection for RNA Biomarkers for TBI Diagnostics

Log Number 13212004 Annual - Year One Progress Report – September 30, 2015

Award Number W81XWH-14-2-0192



PI: Michael J. Heller

Org: University of California San Diego

Award Amount: \$ \$1,871,874.00

**Study/Product Aim(s)** - Most of the year one goals not related to final IRB approval and use of TBI samples have been accomplished. While our milestone for obtaining the UCSD IRB was achieved (May 2015), the IRB has not yet been approved by HRPO-ORP-USAMRMC. Nevertheless, we successfully demonstrated the basic capability of our DEP technology for the isolation of glioblastoma exosomes (containing ccf-RNA) from 50 mL of un-diluted plasma in 20-30 minutes. We then showed tri-color fluorescent detection of the isolated exosomes (red fluorescence), ccf-RNA (green fluorescence) and ccf-DNA (blue fluorescence). Finally, glioblastoma-specific mRNAs for EGFRvIII and b-actin biomarkers were identified by RT-PCR carried out on ccf-RNA from the exosomes. Results represent a key achievement for the first year's work.

**Approach** - Overall project goal is to demonstrate that high conductance dielectrophoretic (HC-DEP) devices and technology can be used to carry out rapid isolation and detection of traumatic brain injury (TBI) ccf-RNA (mRNA, miRNA) and other biomarkers from blood, plasma and serum.

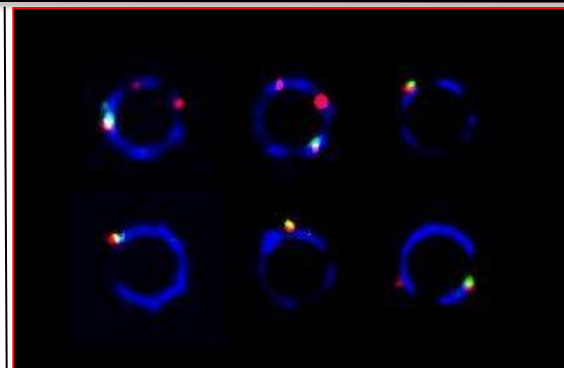


Figure 1 - Multi-color fluorescence image analysis of exosomes, ccf-RNA and DNA isolated from plasma by DEP. Shows six micro-electrodes, where blue is DNA stained with DAPI, red shows the stained exosomes and green shows RNA stained with RNA Select dye.

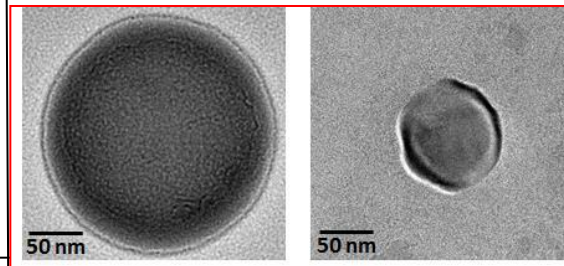


Figure 2 – Shows TEM images of ccf-RNA containing glioblastoma exosomes recovered from cell culture media. The sizes ranged from 50 to 100 nm.

Activities Year 1 (10/14-09/15)	Q-1	Q-2	Q-3	Q-4
First Specific Aim & Tasks:	Milestone 1			
Second & Third Specific Aim & Tasks: "Completed with glioblastoma samples"	Milestone 2 & 5			
Completed IRB and UCSD approval	Milestone 3			
Fourth Specific Aim & Tasks (Raytheon)	Milestone 4			
<b>Estimated Budget (\$K)</b>	<b>\$225</b>	<b>\$450</b>	<b>\$675</b>	<b>\$900</b>

**Year 1 Goals/Milestones** - Carry out and optimize RT and qPCR reactions, and test PCR primers on RNA spiked samples, and glioblastoma/exosome samples completed. **Second & Third Specific Aim & Tasks/Milestones** completed using glioblastoma exosome samples.

- Have received UCSD approval for project IRB ( May 21, 2015 )
- Have responded to IRB information requests by HRPO (ORP/USAMRMC) (September 18, 2015)

**Comments/Challenges/Issues/Concerns**  
Since our IRB has not yet been approved by HRPO (ORP/USAMRMC) we have not been able to work on or collect TBI samples. As soon as IRB is approved we can immediately start work on the related goals.

**Budget Expenditure to Date**  
Projected Expenditure: ~\$900,000.00  
Actual Expenditure: **On Track**

## 9. APPENDICES

For submission to ACS Nano Journal

### Recovery of Exosomes Containing Circulating Cell-Free RNA from Human Plasma Using High Conductance Dielectrophoresis

Stuart Ibsen<sup>1</sup>, Jennifer Wright<sup>1</sup>, Sejung Kim<sup>1</sup>, Seo-Yeon Ko<sup>1</sup>, Jiye Ong<sup>1</sup>, Sareh Manouchehri<sup>2</sup>, Johnny Akers<sup>3</sup>, Clark Chen<sup>3</sup>, and Michael Heller<sup>1</sup>

<sup>1</sup>Department of Nanoengineering, University of California San Diego, La Jolla, CA 92093 USA1

<sup>2</sup>Department of Bioengineering, University of California San Diego, La Jolla, CA 92093 USA1

<sup>3</sup>Moore's Cancer Center, University of California San Diego, La Jolla, CA 92093 USA

#### Abstract

Circulating cell-free (ccf) RNA is an important biomarker that can yield valuable information about cancer and other disease states. Most RNA that exists for any significant period of time in circulation is generally contained or encapsulated in protein-lipid exosome or other extracellular vesicle (ECV) complexes that protect it from endogenous RNase activity in the blood. The small size and low density of the exosomes and ECVs makes their isolation from blood samples a significant challenge that requires large sample volumes and long periods of ultracentrifugation and other processing. Here we demonstrate for the first time the successful use of an electrokinetic technique to rapidly recover RNA encapsulated in exosomes from small sample volumes of human plasma. In this study, exosomes produced by a glioblastoma cell line (U87-EGFRvIII) were spiked into undiluted human plasma samples. A newly designed high conductance dielectrophoretic (DEP) microfluidic device containing a microelectrode array was used to rapidly isolate spiked exosomes from 50  $\mu$ l of plasma. When an AC field is applied the exosomes preferentially concentrate into the DEP high-field region around the microelectrodes in 15-20 minutes. A buffer wash was then used to remove the bulk plasma materials from the device, while the exosomes remained concentrated on the microelectrodes. The complete process (adding sample, applying the DEP field, and washing) allowed recovery of exosomes in about 30 minutes. RNA was detected by fluorescent staining in about 30% of the exosomes. RT-PCR analysis of the ccf-RNA from exosomes showed presence of both a general housekeeping mRNA ( $\beta$ -actin) and mRNA for the cancer-specific EGFRvIII mutation produced by the glioblastoma cells. Control plasma samples without exosomes did not show the presence of either of these two mRNAs. These results demonstrate a proof of concept for DEP streamlining the recovery process for exosomes and associated ccf-RNA from human plasma, by significantly reducing the time and number of processing steps and ultimately improving the yield of viable RNA for subsequent analysis.

## Introduction

Circulating cell-free (ccf) RNA that is released by cells into the blood circulation contains valuable information on potential disease states within the body [1-3]. Since many of the RNAs are specific to the given tissue or cell type, they can also be used for tissue/cell identification [2]. Ccf- RNA can be secreted by cells that are healthy, in a diseased state, undergoing apoptosis, or undergoing necrotic lysis [4]. Because free RNA in the blood is rapidly destroyed by the high levels of endogenous RNase activity [5, 6], the RNA that is present is generally encapsulated and protected within exosomes or extracellular vesicles (ECV) [2, 3, 7]. Exosomes are small lipid/protein vesicles about 40-100 nm in diameter that are actively secreted by cells and enter systemic circulation [8]. Before release, the cells often package nucleic acids and proteins that are produced by the cell into the exosome [8-10].

Exosomes and the associated ccf-RNA need to be purified from the sample before analysis because of the RNase activity and plasma components inhibiting the RT-PCR process. Due to their small size and low density the isolation of exosomes from other components in the blood is a significant challenge. The current state of the art exosome recovery techniques make use of overnight incubations with exosome precipitation kits [10] or extensive ultracentrifugation steps that can range from 1.5 hours [3], to 5 hours [11] to even overnight [12], in addition to the time taken for additional filtration steps and sample handling. These time consuming methods with their extensive processing steps can also damage the exosomes and reduce the overall collection efficiency. Other recovery methods include filtration that does not separate out plasma proteins [13], and immunoaffinity isolation with magnetic beads that requires significant dilution of the plasma sample with PBS beforehand [14]. Thus, a major challenge exists in being able to design a recovery method that works with undiluted plasma, reduces mechanical damage to the exosomes, and reduces the long processing times between sample collection and RNA isolation. Achieving these reductions will keep the exosomes and their RNA contents in a more intact state allowing for a more accurate and sensitive analysis of the RNA present in circulation [15].

To address these many challenges for exosome/RNA isolation, we present a new method for isolation of exosomes directly from undiluted human plasma with a simple three-step minimal processing protocol. The exosomes are rapidly separated from the bulk plasma, allowing RT-PCR to be successfully performed on the extracted RNA. This method is based on an electrokinetic separation technique called dielectrophoresis (DEP). DEP uses an alternating electric field to create a force that causes preferential separation between the exosomes and the surrounding bulk plasma that is based on the difference between the dielectric properties of the material making up the exosomes and the surrounding plasma fluid. The dielectric constants of the material indicate how fast charges will move through the material in response to a change in the external electric field. The charges reorient themselves at different speeds in the plasma and in the particle creating monetary dipoles across the particle. In a non-uniform electric field these dipoles create a force that pulls the particle into the high intensity region of the electric field. An enabling electrode array chip based technology now allows for this DEP recovery process to be performed in high conductance solutions [16-19] such as blood plasma and serum [19-21]. These microelectrode arrays contain a microfluidic channel that brings the plasma sample into contact with the electrodes that create the electric field. The highest electric field strength exists around the edge of each circular electrode and is where the particles collect. In previous work, we successfully used DEP to recover liposome based drug delivery nanoparticles from undiluted human plasma [22] and we hypothesized that this technique could also be used on exosomes that have been spiked into plasma.

## **Methods**

Exosomes used in these experiments were isolated from the cell culture media of cultured glioblastoma U87–EGFRvIII neuronal cells showing an epidermal growth factor receptor mutation. These cells have been shown to naturally produce exosomes[23] and excrete them into the cell culture media. These exosomes were isolated from the cells as described below and spiked into undiluted human plasma samples for DEP isolation.

### **Exosome free media preparation**

Exosome-depleted medium was prepared by ultracentrifugation of DMEM supplemented with 20% FBS at 120,000 x g for 18 hours at 4°C. The medium was then diluted to a final concentration of 10% FBS and used to culture cell lines as described.

### **Exosome isolation from cell culture media**

U87(MG)-EGFRvIII cells were cultured to 60-70% confluency, the standard culture medium was replaced with exosome depleted medium. The cells were cultured for an additional 72 hours before exosome collection from the cell-free supernatants by differential centrifugation. Conditioned media was first centrifuged at 300 x g for 10 minutes to remove cellular debris. The supernatant was collected and further centrifuged at 2,000 x g for 20 minutes. The resultant supernatant was then transferred to ultracentrifuge tubes for ultracentrifugation at 120,000 x g for 2 hours. The supernatant was discarded and the exosome pellets were re-suspended in PBS for storage at -80°C. All centrifugation steps were performed at 4°C

### **Exosome labeling**

U87(MG)-EGFRvIII derived exosomes were labeled with PKH26. (PKH26 Red Fluorescent Cell Linker Mini Kit for General Cell Membrane Labeling, Sigma-Aldrich, St. Louis, MO). Isolated exosomes were diluted to 1 mL with Diluent C from the kit prior to mixing with freshly prepared PKH26 solution (4 µL of PKH26 dye was added to 1 mL of Diluent C). The samples were mixed gently for 4 min before 2 mL of 1% BSA was added to bind the excess dye. 12 mL of PBS was added to the mixture and the labeled exosomes were pelleted by ultracentrifuge at 120,000 x g for 2 hours. The supernatant was removed, and the pellets were washed with 16 mL of PBS and centrifuged at 120,000g for 2 hours at 4 °C. A control sample that was run through the labeling process , but did not contain any exosomes, showed minimal presence of red fluorescent particles after the wash showing that red particles observed in the labeled samples were mostly exosomes. The labeled exosome sample had a final concentration of  $5 \times 10^9$  particles/mL as determined by a NanoSight particle tracking system.

## **Preparation of exosome spiked human plasma**

Normal human plasma samples were purchased from Sigma. The exosomes collected from the U87-EGFRvIII cells were then spiked into human plasma at a 1:9 dilution ratio.

## **DEP isolation and recovery of the exosomes**

The DEP recovery of the exosomes took place in a three step process:

Step 1: A 30  $\mu$ L sample of the spiked plasma samples were immediately placed on the DEP microfluidic device after spiking. The electrodes were powered with a 10 Vpp, 15 KHz signal for 10 min. This was sufficient time to collect the exosomes.

Step 2: With the DEP field still on, the chip was washed with a 1X TE buffer at 20  $\mu$ L/min for 10 minutes to remove the bulk plasma signal.

Step 3: The DEP field was then switched to 3 pulses of 0.5 s duration at 5 Hz and 10 Vpp. This reversed the DEP force and pushed the collected exosomes into the bulk wash buffer, allowing for collection from the chip for further analysis.

The total time required from adding the spiked plasma sample to the chip to recovering the purified exosomes was 30 min.

## **TEM analysis**

### Exosome negative staining

The exosome dispersion was diluted in PBS (20X v/v). A small drop of the diluted exosome solution (5  $\mu$ L) was placed on a TEM imaging grid and the exosomes were allowed to adhere to the carbon film for 5 minutes. The carbon-coated TEM grid was treated with a glow discharge using an Emitech K350 for a minute to make it hydrophilic. Then, 20 drops of DI water was applied to the grid in order to remove any unbound exosomes and PBS to prepare for the staining procedure. A 5  $\mu$ L drop of 1% of uranyl acetate solution was placed onto the grid and flicked off. This was repeated 2 times. The remaining 1% of uranyl acetate solution was removed by absorbing the stain from the edge of the grid with a wedge of filter paper. The grid was dried in air for TEM imaging.

### TEM parameters

The exosomes samples were analyzed with a transmission electron microscope (TEM, FEI Tecnai G2) using an accelerating voltage of 200 kV.

## **SEM analysis**

### Sample drying preparation

The DEP chips were run as described above without using the sample push off for recovery thereby leaving the collected material intact on the electrode edges. The chips were then placed in a -80°C freezer which quickly froze the 35  $\mu$ L of water in the chip. The whole chip was placed in a lyophilizer overnight to remove the water leaving the shape of the collected material preserved for analysis.

A second air drying technique was used to prepare the chips for SEM analysis where the chips were left out overnight to dry. This method of evaporation allowed the collected material to collapse into a thin film when completely dry. Polystyrene based (Fluospheres 110 nm in diameter) were spiked into the plasma sample to help identify the region of collection around each electrode.

#### SEM parameters

The dried chips were coated with iridium for 7 seconds. The chips were analyzed with an environmental scanning electron microscope (ESEM, Phillips XL30) operated at 10 kV.

#### **RT-PCR and PCR analysis**

The exosomes recovered from DEP isolation were lysed to release the RNA contents by running them through a miRCURY RNA Isolation Kit – Biofluids (Exiqon Life Sciences) in order to release the RNA from protected material and allow access for further analysis. The purified RNA was then used in an RT-PCR reaction using random hexamers and SuperScript III Reverse Transcriptase (Thermo Fisher). After the cDNA was obtained, it was used in both qPCR reactions for detection of  $\beta$ -actin and end-point PCR reactions for detection of EGFRvIII.

#### Results and Discussion

Exosomes that were recovered from the cell culture media were analyzed using transmission electron microscopy and representative images are shown in Figure 1.

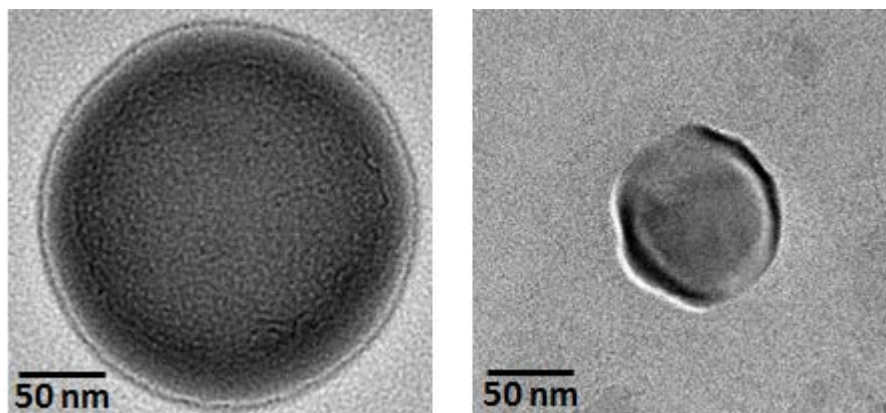
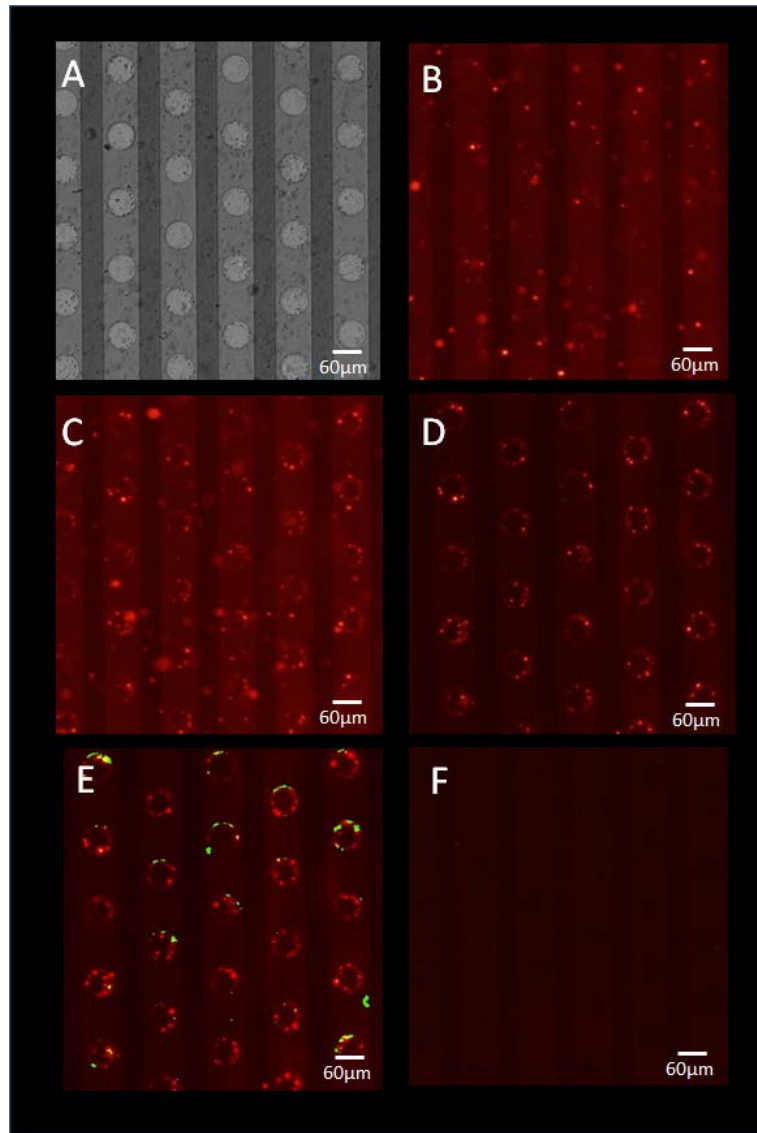


Figure 1 – Example exosomes that were recovered from the cell culture media and analyzed using TEM. The sizes ranged from 50 to 100 nm.

The exosomes that were spiked into undiluted human plasma were successfully recovered using the DEP technique within 30 min. Figure 2 shows images taken at different stages of the DEP isolation process. The bright-field image of the DEP chip surface shows the light colored circular electrodes that create the non-uniform electric field (Figure 2a). The fluorescently labeled exosomes were visible as red coloration in the bulk plasma sample and larger aggregates of exosomes were visible as red spots (Figure 2b). The non-uniform electric field strength is highest around the edges of the electrode, which is where the exosomes concentrate after 10 min of DEP field application (Figure 2c). The DEP force held the exosomes in place while a 1X TE buffer wash removed the bulk plasma and uncollected exosomes (Figure 2d). To indicate the presence of RNA in the exosomes samples the RNA-specific stain, RNA Select, was introduced into the wash buffer. RNA Select is membrane permeable and can cross the exosome membrane to stain RNA that might be inside. The exosomes were allowed to incubate for 10 min with the RNA Select before the excess dye was washed away. Exosomes that showed the RNA Select accumulation indicate that they contained RNA. Figure 2e shows the composite image with the RNA Select dye in green overlaid with the red exosomes. It can be seen that not all of the exosomes stained for RNA content. The reverse DEP pulse was then applied to the purified exosomes, pushing them off the surface of the DEP chip and into the bulk wash buffer for collection. Figure 2f shows an image taken after the exosomes were recovered demonstrating that the vast majority of the purified exosomes were removed from the chip for analysis.



**Figure 2** – Images at the different stages of DEP purification and recovery of spiked exosomes from undiluted human plasma. **A** - Bright-field image of the DEP chip surface. Each of the circles is an individual electrode. The electric field is strongest at the edges of the electrode and is also where the DEP strength is the highest. **B** - A fluorescent view of the surface of the DEP chip. The exosomes have been labeled with the red PKH26 dye. Larger aggregates of the exosomes are visible as red dots. **C** - After 10 min. of DEP field application, the exosomes are collected around the edge of the electrodes, forming a fluorescent ring. **D** - The bulk plasma and uncollected exosomes are removed with a 10 min. wash with 1X TE buffer leaving the captured exosomes in the high DEP field region in place. **E** - The captured exosomes were stained with RNA Select that is specific for RNA and is membrane permeable. The RNA Select is shown in green in this composite image. Only a fraction of the exosomes actually stained for RNA content. **F** - The isolated exosomes were pushed off the surface of the chip by reversing the DEP force and were recovered for further analysis.

The DEP collection process is also capable of simultaneously pulling spiked high molecular weight DNA down to the electrode edges as well as exosomes containing RNA in undiluted plasma as shown in Figure 3.

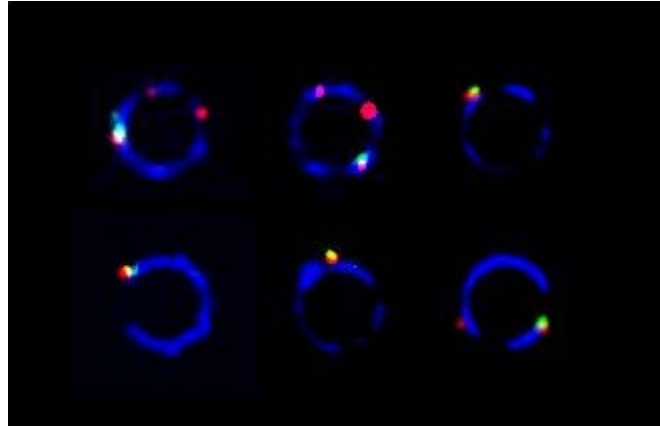
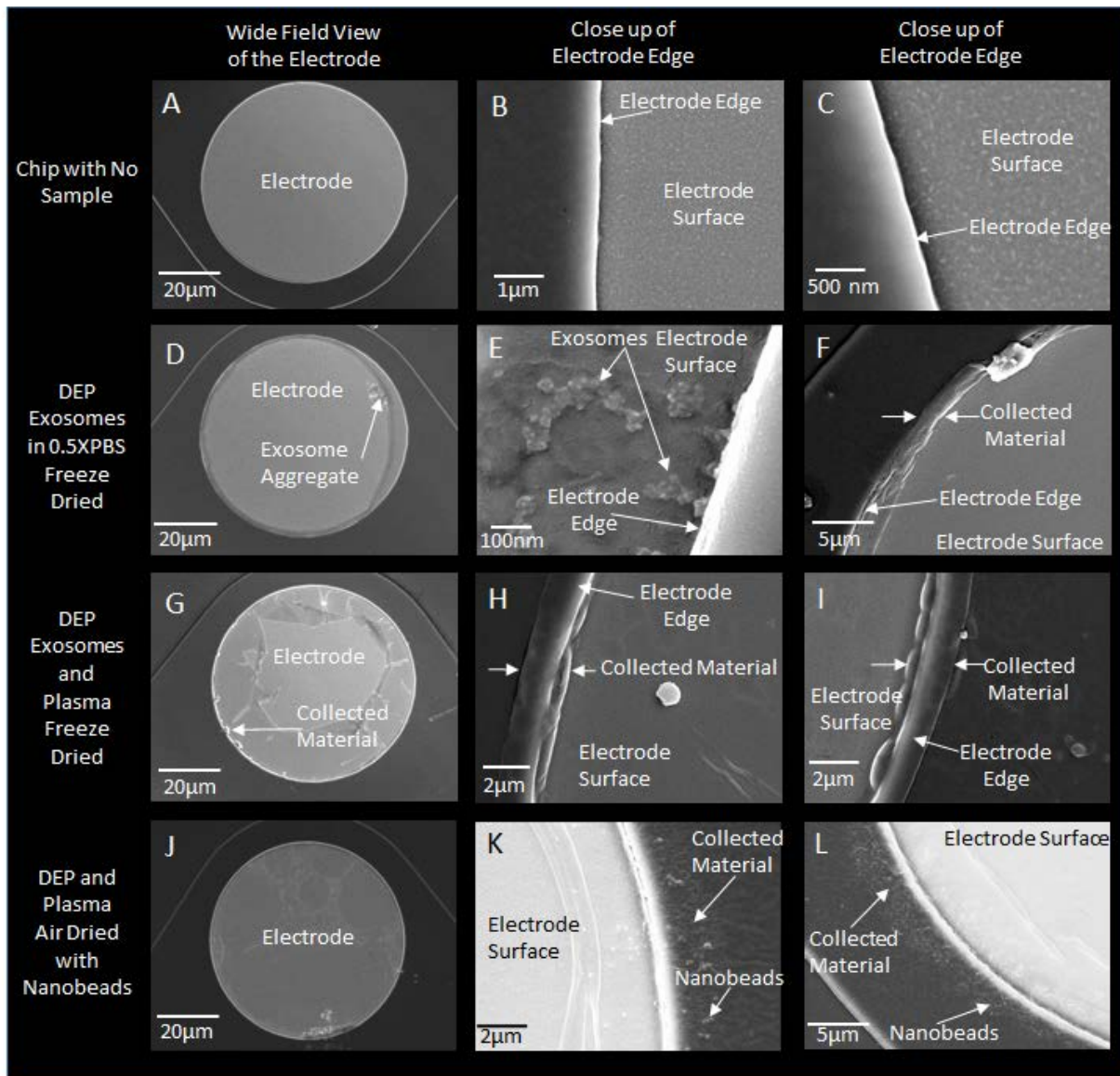


Figure 3 – High molecular weight DNA that was spiked into the plasma sample was also shown to be simultaneously pulled down to the edge of the electrodes along with the exosomes. Here 6 representative electrodes are shown where blue shows the DNA stained with DAPI, red shows the exosomes, and green shows where RNA Select stained the exosomes for RNA content. As observed in Figure 2, not all of the exosomes co-stained for RNA content.

The surface of the DEP chip was then analyzed using scanning electron microscopy (SEM) to visualize the location of the collected material (Figure 4). Polystyrene nanobeads (100 nm diameter) were spiked into the plasma to help identify the collection region on the surface of the chip. The DEP collection was performed and the sample was washed to remove the bulk plasma. The chip was then dried for SEM analysis using both freeze drying and air drying techniques. These images show the surface characteristics of the collected material in the high field region around the electrode edges.



**Figure 4** – Scanning electron microscopy images of the DEP electrode array surface before and after DEP collection from human plasma and washing. **A** - An electrode from a chip before it has been exposed to plasma. **B and C** - A magnified view of the edge between the electrode and the silica surface of the chip showing no collected material. **D** - An electrode after collection and washing of exosomes from 0.5X PBS buffer with a freeze drying preparation. The hydrogel layer on the surface of the electrode has separated from the platinum electrode underneath creating a surface texture. **E** - Magnified view of the electrode edge showing the collection of particles from the exosome sample. **F** - Another view of collected material from the exosome sample. This material most likely includes proteins and lipids from the original cell culture media **G** - Electrode after collection and washing of exosomes from a spiked undiluted human plasma sample. The hydrogel layer has been ruptured possibly from the freeze drying process. **H and I** - Magnified view of the electrode edge. Material from the plasma including DNA and the exosomes (Figure 3) are shown here collected together as the curved smooth surface of material indicated between the arrows. This material hides the exosomes within it. The freeze drying process has preserved the original shape of the collected material. **J** - Surface of the electrode after collection of 110

diameter polystyrene nanobeads from undiluted human plasma prepared using an air drying process. **K and L** - A magnified view of the electrode edge. When allowed to air dry the collected material collapsed into a thin film showing the nanobeads within it.

The removal of the bulk plasma allowed RT-PCR followed by PCR to be successfully applied to the recovered exosome samples to analyze the RNA content. The U87 cell line has a specific EGFRvIII mutation that PCR primers have been developed to detect. The presence of RNA in the recovered exosomes that contains this cell-specific mutation was confirmed using RT-PCR followed by endpoint PCR as shown in Figure 5.

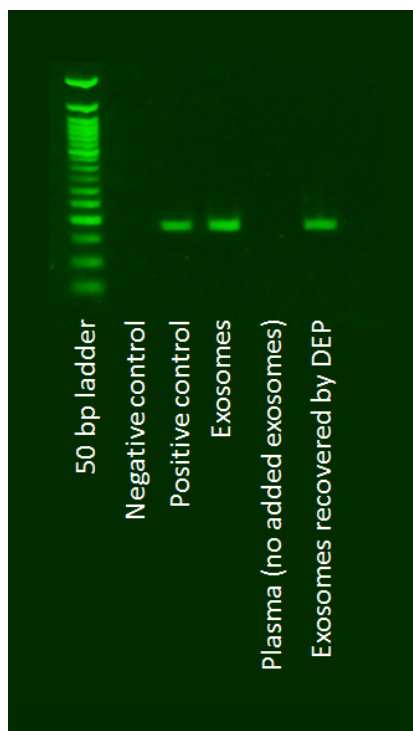


**Figure 5** – Gel analysis of RT-PCR followed by endpoint PCR performed on the DEP recovered exosomes using primers specific for the EGFRvIII mutation expressed by the U87 cell line. The negative control and the plasma from a normal healthy donor that did not have exosomes spiked into it did not show any RNA coding for the EGFRvIII mutation. The DEP method recovered sufficient amounts of exosomes to see RNA content and shows that RNA specific for the cell line of interest can be detected.

RT-PCR primers for the general housekeeping protein  $\beta$ -actin were also used to see if RNA coding for additional proteins was present in the DEP recovered exosomes. The presence of RNA coding for  $\beta$ -actin was confirmed using qPCR as shown in Figure 6.

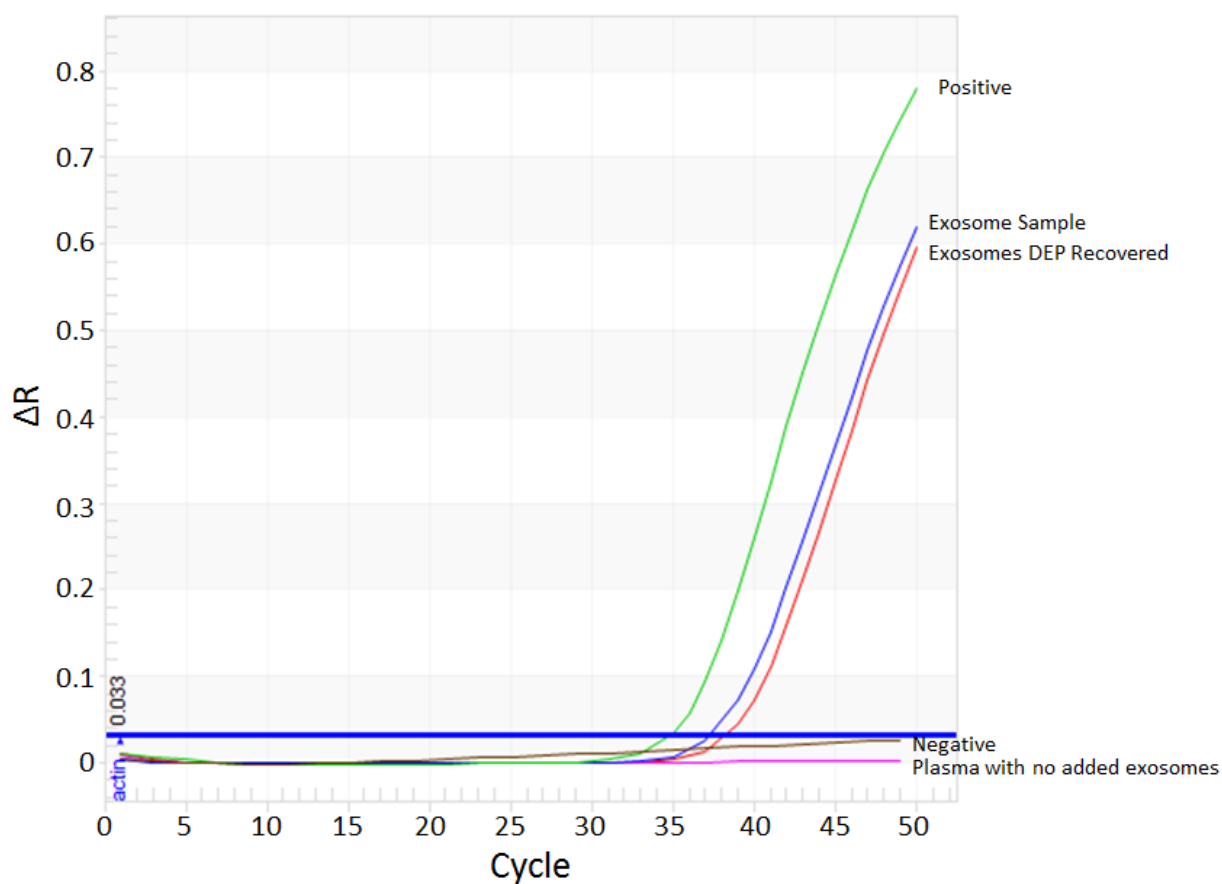
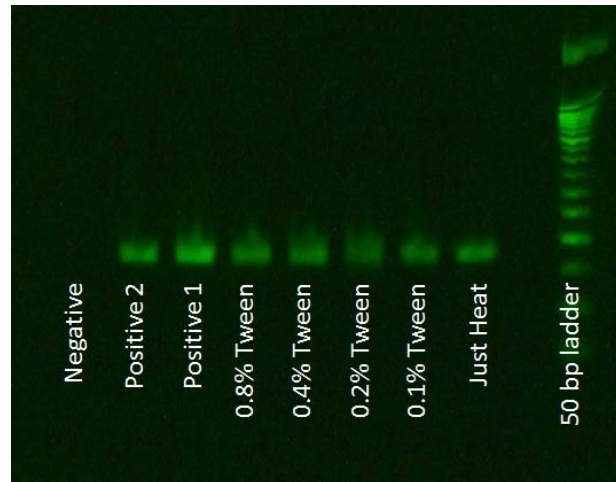


Figure 6 – RT-PCR followed by qPCR analysis using RNA primers for  $\beta$ -actin from exosomes recovered using DEP. The exosome sample before spiking into the plasma came up showing that  $\beta$ -actin was present in the exosome sample. Two replicate samples of exosomes recovered for undiluted plasma using the DEP technique show the presence of RNA coding for  $\beta$ -actin.

The data presented above required a lysis step to isolate/purify the RNA from the DEP-recovered exosomes so it would be available for RT-PCR. The lysis was performed by running these samples through an RNA isolation kit (Exiqon kit). We also showed that the RNA could be released from the exosomes using heat as well as surfactants that can help to disrupt the exosome membrane but not interfere with the RT-PCR process (Figure 7). Performing RT-PCR directly on the recovered exosome samples increases the speed with which the RNA can be analyzed and streamlines the process to avoid extra steps where RNA could be lost.



**Figure 7** - Gel analysis of RT-PCR followed by endpoint PCR performed on the exosomes using primers specific for the EGFRvIII mutation expressed by the U87 cell line. These exosomes were not lysed by the use of an Exiqon kit but rather the RNA was released by heating the exosomes and using tween20 surfactant in increasing concentrations to disrupt the exosome membrane. These techniques were successful in releasing the rare EGFRvIII coding RNA from the exosomes for analysis.

## Conclusion

Our DEP-based recovery method was able to successfully recover spiked exosomes from undiluted human plasma samples. Sufficient exosome quantities were recovered to allow RT-PCR detection of cell-specific mRNA for EGFRvIII and general housekeeping mRNA for  $\beta$ -actin. The DEP recovery method requires only 3 steps and is completed within 30 minutes. This allows freshly collected plasma samples to be rapidly analyzed minimizing RNA degradation. The DEP method is significantly faster than any of the current state of the art ultracentrifugation methods. The faster processing time should also increase the quantity and quality of the RNA recovered for analysis. The DEP microarray (chip) device requires only a small 30  $\mu$ L sample volume, which is important for precious and rare samples where it is desirable to preserve as much of the original sample as possible. The unique ability to hold the exosomes in place allowed for the RNA content within the exosomes to be monitored by fluorescent staining with RNA Select dye. The RNA fluorescent staining showed about 30% of the exosomes contained RNA.

## Acknowledgements

This work was supported by Award Number W81XWH-14-2-0192 from the Defense Medical Research and Development Program and U.S. ARMY MEDICAL RESEARCH ACQUISITION ACTIVITY (USAMRAA).

## References

[1] Zhou H, Xu W, Qian H, Yin Q, Zhu W, Yan Y. Circulating RNA as a novel tumor marker: an in vitro study of the origins and characteristics of extracellular RNA. *Cancer letters*. 2008;259:50-60.

- [2] Mitchell PS, Parkin RK, Kroh EM, Fritz BR, Wyman SK, Pogosova-Agadjanyan EL, et al. Circulating microRNAs as stable blood-based markers for cancer detection. *Proceedings of the National Academy of Sciences*. 2008;105:10513-8.
- [3] Gallo A, Tandon M, Alevizos I, Illei GG. The majority of microRNAs detectable in serum and saliva is concentrated in exosomes. *PloS one*. 2012;7:e30679.
- [4] Moldovan L, Batte K, Wang Y, Wisler J, Piper M. Analyzing the circulating microRNAs in exosomes/extracellular vesicles from serum or plasma by qRT-PCR. *Circulating MicroRNAs: Springer*; 2013. p. 129-45.
- [5] Tsui NB, Ng EK, Lo YD. Stability of endogenous and added RNA in blood specimens, serum, and plasma. *Clinical chemistry*. 2002;48:1647-53.
- [6] Houseley J, Tollervey D. The many pathways of RNA degradation. *Cell*. 2009;136:763-76.
- [7] Kosaka N, Yoshioka Y, Hagiwara K, Tominaga N, Ochiya T. Functional analysis of exosomal microRNA in cell-cell communication research. *Circulating MicroRNAs: Springer*; 2013. p. 1-10.
- [8] Mathivanan S, Ji H, Simpson RJ. Exosomes: extracellular organelles important in intercellular communication. *Journal of proteomics*. 2010;73:1907-20.
- [9] Simpson RJ, Jensen SS, Lim JW. Proteomic profiling of exosomes: current perspectives. *Proteomics*. 2008;8:4083-99.
- [10] Huang X, Yuan T, Tschannen M, Sun Z, Jacob H, Du M, et al. Characterization of human plasma-derived exosomal RNAs by deep sequencing. *BMC genomics*. 2013;14:319.
- [11] Caby M-P, Lankar D, Vincendeau-Scherrer C, Raposo G, Bonnerot C. Exosomal-like vesicles are present in human blood plasma. *International immunology*. 2005;17:879-87.
- [12] Melo SA, Luecke LB, Kahlert C, Fernandez AF, Gammon ST, Kaye J, et al. Glypican-1 identifies cancer exosomes and detects early pancreatic cancer. *Nature*. 2015.
- [13] Grant R, Ansa-Addo E, Stratton D, Antwi-Baffour S, Jorfi S, Kholia S, et al. A filtration-based protocol to isolate human plasma membrane-derived vesicles and exosomes from blood plasma. *Journal of immunological methods*. 2011;371:143-51.
- [14] Kalra H, Adda CG, Liem M, Ang CS, Mechler A, Simpson RJ, et al. Comparative proteomics evaluation of plasma exosome isolation techniques and assessment of the stability of exosomes in normal human blood plasma. *Proteomics*. 2013;13:3354-64.
- [15] Botling J, Edlund K, Segersten U, Tahmasebpour S, Engström M, Sundström M, et al. Impact of thawing on RNA integrity and gene expression analysis in fresh frozen tissue. *Diagnostic Molecular Pathology*. 2009;18:44-52.
- [16] Krishnan R, Dehlinger DA, Gemmen GJ, Mifflin RL, Esener SC, Heller MJ. Interaction of nanoparticles at the DEP microelectrode interface under high conductance conditions. *Electrochemistry communications*. 2009;11:1661-6.
- [17] Sonnenberg A, Marciniak JY, Krishnan R, Heller MJ. Dielectrophoretic isolation of DNA and nanoparticles from blood. *Electrophoresis*. 2012;33:2482-90.
- [18] Sonnenberg A, Marciniak JY, McCanna J, Krishnan R, Rassenti L, Kipps TJ, et al. Dielectrophoretic isolation and detection of cfDNA nanoparticulate biomarkers and virus from blood. *Electrophoresis*. 2013;34:1076-84.
- [19] Krishnan R, Sullivan BD, Mifflin RL, Esener SC, Heller MJ. Alternating current electrokinetic separation and detection of DNA nanoparticles in high conductance solutions. *Electrophoresis*. 2008;29:1765-74.
- [20] Sonnenberg A, Marciniak JY, Skowronski EA, Manouchehri S, Rassenti L, Ghia EM, et al. Dielectrophoretic isolation and detection of cancer related circulating cell free dna biomarkers from blood and plasma. *Electrophoresis*. 2014;35:1828-36.

[21] Sonnenberg A, Marciniak JY, Rassenti L, Ghia EM, Skowronski EA, Manouchehri S, et al. Rapid Electrokinetic Isolation of Cancer-Related Circulating Cell-Free DNA Directly from Blood. *Clinical chemistry*. 2013;60:500-9.

[22] Ibsen S, Sonnenberg A, Schutt C, Mukthavaram R, Yeh Y, Ortac I, et al. Recovery of Drug Delivery Nanoparticles from Human Plasma Using an Electrokinetic Platform Technology. *Small*. 2015.

[23] Skog J, Würdinger T, van Rijn S, Meijer DH, Gainche L, Curry WT, et al. Glioblastoma microvesicles transport RNA and proteins that promote tumour growth and provide diagnostic biomarkers. *Nature cell biology*. 2008;10:1470-6.